OCEAN DRILLING PROGRAM

LEG 202 SCIENTIFIC PROSPECTUS

SOUTHEAST PACIFIC PALEOCEANOGRAPHIC TRANSECTS

Dr. Alan C. Mix
Co-Chief Scientist
College of Oceanic and
Atmospheric Sciences
Oregon State University
104 Ocean Administration Building
Corvallis OR 97331-5503
USA

Dr. Ralf Tiedemann
Co-Chief Scientist
GEOMAR Research Center
for Marine Geosciences
Wischhofstrasse 1-3,
24148 Kiel
Germany

Dr. Jack Baldauf
Deputy Director of Science Operations
Ocean Drilling Program
Texas A&M University
1000 Discovery Drive
College Station TX 77845-9547
USA

Dr. Peter Blum
Leg Project Manager and Staff Scientist
Ocean Drilling Program
Texas A&M University
1000 Discovery Drive
College Station TX 77845-9547
USA

November 2001

PUBLISHER'S NOTES
Material in this publication may be copied without restraint for library, abstract service, educational, or personal research purposes; however, this source should be appropriately acknowledged.

Ocean Drilling Program Scientific Prospectus No. 102 (October 2001)

Distribution: Electronic copies of this publication may be obtained from the ODP Publications homepage on the World Wide Web at: http://www-odp.tamu.edu/publications

This publication was prepared by the Ocean Drilling Program, Texas A&M University, as an account of work performed under the international Ocean Drilling Program, which is managed by Joint Oceanographic Institutions, Inc., under contract with the National Science Foundation. Funding for the program is provided by the following agencies:

Australia/Canada/Chinese Taipei/Korea Consortium for Ocean Drilling
Deutsche Forschungsgemeinschaft (Federal Republic of Germany)
Institut National des Sciences de l'Univers-Centre National de la Recherche Scientifique (INSU CNRS; France)
Ocean Research Institute of the University of Tokyo (Japan)
National Science Foundation (United States)
Natural Environment Research Council (United Kingdom)
European Science Foundation Consortium for Ocean Drilling (Belgium, Denmark, Finland, Iceland, Ireland, Italy, The Netherlands, Norway, Portugal, Spain, Sweden, and Switzerland)
Marine High-Technology Bureau of the State Science and Technology Commission of the People's Republic of China

Technical Editors: Karen K. Graber and Lorri L. Peters

ABSTRACT

The scientific objectives of Leg 202 are paleoceanographic: to assess climate and oceanographic changes in the southeast Pacific over Neogene time. The drilling experiment contains three major elements, to probe the climate system at three different but compatible scales: tectonic (millions of years), orbital (tens to hundreds of thousands of years), and millennial (thousands of years). On these three timescales, drilling will test a broad set of hypotheses on the following:

1. Linkages between high- and low-latitude climate changes in the Southern Hemisphere via the Eastern Boundary Current on orbital and millennial scales;
2. The response of the South Pacific Ocean to major tectonic and climatic events, such as the opening of the Drake Passage (creating a circumpolar current), closing of the Panama Isthmus (separating the Atlantic and Pacific Oceans), the uplift of the Andes Mountains (modifying wind systems), and major expansion of ice sheets in the high latitudes of the Southern and Northern Hemispheres at different times; and
3. The role of biological productivity and physical ventilation of water masses in modifying subsurface water masses near the eastern boundary, as reflected in biotic and geochemical composition of nutrients and oxygen in subsurface water masses.

Our operational goals are to maximize the depth range of sites to sample different parts of the water column, to place the sites reasonably close to South and Central America to maximize sedimentation rates, and to assure good Neogene coverage of the Eastern Boundary Currents in a latitudinal transect, while avoiding as much as possible the influence of local tectonic deformation and input of turbidites. Some sites target low sedimentation rates to obtain long sequences of climate change in early Neogene time that are not subject to severe burial diagenesis. Others target higher sedimentation rates to assess orbital-scale climate oscillations at a resolution suitable for tuning of timescales and examination of changing responses to orbital forcing in late Neogene time. Finally, a few sites target rapidly accumulating sediments near the equator and in the midlatitudes to assess millennial-scale climate oscillations of the Southern Hemisphere. In all cases, we plan to recover and verify continuous sedimentary sections by drilling multiple advanced piston coring (APC) holes at each site. We expect to find a good record of biogenic sediment components, geochemical tracers of surface and subsurface water masses, and in some sites a record of terrigenous sediment components in hemipelagic and pelagic sediments.

BACKGROUND

The paleoceanography of the southeast Pacific Ocean off the coast of South America has received little attention in past drilling experiments and remains essentially unknown to this day. The Deep Sea Drilling Project (DSDP) did not visit the western margin of South America and provided only two sites in the Peru Basin (Sites 320 and 321). The Ocean Drilling Program (ODP) examined 10 sites on the Peru Margin during Leg 112, which provided key evidence for sedimentation and geochemical processes in this productive and nearly anoxic sediment system. ODP Leg 141 examined the tectonics of the Chile Triple Junction and got a first look at sediments at five sites on the margin of southern Chile, but these sites provided relatively little material suitable for paleoceanographic studies. Leg 202 seeks to remedy this situation by examining a broad range of sites off South America, from central Chile to the equator (Fig. 1; Tables 1, 2). Depth and latitudinal transects of sites will facilitate study of changes in vertical ocean circulation and surface ocean processes as they change through time.

Oceanographic Setting

Modern subsurface circulation of the southeast Pacific is illustrated in water mass properties in profiles of dissolved oxygen, phosphate, and salinity in a meridional transect of the eastern Pacific (Fig. 2). Bottom water presently enters eastern basins of the South Pacific from the south, below 3-km water depth (Lonsdale, 1976). After transiting north, accumulating nutrients and losing oxygen in the North Pacific, much of the Pacific Deep Water exits as a middepth southward flow between 1 and 3 km. This middepth outflow and its importance to Pacific (and global) distributions of nutrients has been known for nearly 30 yr (Reid, 1973). But how it changes through time remains a mystery. Recent debate centers on the role of Southern Hemisphere winds in maintaining the global thermohaline circulation (Toggweiler and Samuels, 1993). Much of the advective export of phosphate and nitrate from the Pacific occurs in the southward return flow between 1 and 3 km in the eastern Pacific, where concentrations of these nutrients are highest (Wunsch et al., 1983). Thus, changes in this flow have the potential to change nutrient budgets in the Pacific and global ocean (Berger et al., 1997).

At intermediate water depths, water mass properties of the Pacific Ocean are highly asymmetric. Antarctic Intermediate Water (AAIW) is relatively depleted in phosphate and contains abundant oxygen because it forms in substantial contact with the atmosphere. This combination of processes results in relatively high $\delta^{13}C$ in AAIW (Kroopnick, 1985). At present, AAIW is for the most part restricted to the Southern Hemisphere. North Pacific Intermediate Water (NPIW), which forms in the northwest Pacific with relatively little interaction with the atmosphere (Talley, 1993) contains abundant nutrients, but the NPIW is relatively low in oxygen and has low $\delta^{13}C$. An exceptionally steep property gradient between the southern source and northern source water masses occurs, at present, south of the equator. These intermediate water masses are found in the eastern Pacific, typically at depths of ~500-1000 m.

At the shallow end of the intermediate water (typically a few hundred meters water depth) is the classical oxygen minimum zone (OMZ), driven by degradation of organic matter sinking out of the euphotic zone and modified by ocean circulation (Wyrtki, 1962). North of the equator, the OMZ is extremely intense (<0.2 mL/L O_2) between 200 and 900 m. This broad depth range of this OMZ reflects the presence of NPIW, which is depleted in oxygen because it exchanges relatively little with the atmosphere in its northern source areas, as well as the exceptionally high export of organic matter from productive upwelling systems along the eastern boundary of the Pacific Ocean (Tsuchiya and Talley, 1998). A relatively shallow and abrupt pycnocline below low-salinity surface waters helps to maintain the shallow oxygen minimum north of the equator.

The large pools of oxygen-poor water at intermediate depths in the modern eastern Pacific Ocean (Tsuchiya and Talley, 1998) both north and south of the equator are major sites of denitrification and represent collectively the largest sink for nitrogen in the world's oceans. By acting as governors of the average oceanic nitrate concentration, these regions (along with the Arabian Sea) have the potential to act as climate rheostats by altering the global fertility and, thus, the rate of CO_2 fixation within the sea. Indeed, temporal decreases and increases in export production off northwestern Mexico, off Peru, and in the Arabian Sea do appear to have modulated the oxygen content in upper intermediate depth waters and the consequent intensity of denitrification during the late Quaternary (Codispoti and Christensen, 1985; Ganeshram et al., 1995). Whether or not such variations occurred on a broad scale over long time periods remains an open question. For example, it is unclear whether biological production of the eastern tropical Pacific was higher (Lyle et al., 1988) or lower (Loubere, 2000) than at present during the last ice age.

Near the equator, the OMZ is shallower (300-400 m depth) and oxygen values return to typical deep Pacific values of 1 mL/L by ~700 m depth (Fig. 2). Farther south, off central Chile, a "double" OMZ reflects southward advection of oxygen-depleted waters from the Peru margin at ~200-500 m depth in the poleward-flowing Gunther Undercurrent (GU), above the relatively oxygen-rich AAIW near ~500-1000 m. Pacific Central Water (PCW; of Northern Hemisphere origin) comprises the deeper oxygen minimum from ~1500 to 2000 m depth. Oxygen is slightly higher (and nutrient contents lower) in the deep basin because of the incursion of Circumpolar Deep Water (CPDW) below ~3000 m.

Near-surface waters of the eastern Pacific Ocean also exhibit exceptional spatial variability, reflecting the influence of the Peru (or Humboldt) Current, the largest and most continuous Eastern Boundary Current in the global oceans (Fig. 3). Cool waters of the Peru Current (Fig. 4) are advected northward from Chile to offshore reaches of Peru (Strub et al., 1998). Coastal upwelling off central Peru maintains this cool flow (Toggweiler et al., 1991), and these waters merge to feed the westward-flowing South Equatorial Current, which is in turn maintained by equatorial upwelling as the Equatorial Cold Tongue. On an interannual scale, Liu and Huang (2000) argue based on modern heat budgets that warming in the region over the past 50 yr is related to reduction of the wind-driven advection of cool water off the eastern boundary and that such effects extend even to the western Pacific Ocean. A primary question for ocean drilling is whether long-term variability of the equatorial cold tongue is related to changing character of eastern boundary waters.

Near the equator, east of the Galapagos Islands, the Equatorial Front separates the cold, salty waters of the Peru Current from warmer and fresher tropical waters of the Northern Hemisphere. North of the equator, the Panama Basin region is noted for its extreme warmth (often >30°C), exceptionally low salinity (near 32 practical salinity units [PSU]), and strong shallow pycnocline (typically centered near 20-40 m water depths) (Figs. 4, 5). These features north of the equator reflect high rainfall relative to evaporation (Magaña et al., 1999), which stabilizes the water column and diminishes vertical mixing of heat and other properties. A significant fraction of the net fresh water flux to the Panama Basin originates in the Atlantic Ocean or Caribbean Sea (Jousaumme et al., 1986), so low salinities here reflect the transport of fresh water from the Atlantic to Pacific Basins via the atmosphere. The dynamics of this transport are important because this relatively small transport of fresh water helps to maintain the relatively high salinity of the Atlantic Ocean—a key parameter in maintaining the global thermohaline "conveyor belt" circulation dominated by North Atlantic Deep Water (Zaucker et al., 1994; Rahmstorf, 1995).

The region is highly productive but is significant in the world's oceans for not consuming all nutrients at the sea surface (Fig. 6). High phosphate concentrations in tropical surface waters here (Levitus et al., 1993) are now thought to reflect biological limitations associated with iron or other so-called micronutrients. This is significant because any change in the net nutrient utilization would also cause a change in the net flux of CO_2 and other biologically mediated gases from the sea surface.

Tectonic Setting

Many of the proposed sites are located on bathymetric rises with pelagic or hemipelagic sedimentation. Most are relatively isolated from continental margin turbidites and tectonics by the Peru-Chile Trench or other bathymetric features. Age constraints are based on magnetic lineations. For these estimates, we use the magnetic anomaly age model of Cande and Kent (1995), which is in reasonable agreement with orbitally tuned sedimentary age models of the last 5 m.y. and with radiometric dates at older intervals. Maps of the crustal magnetic lineations, with our proposed sites superimposed, are illustrated as Figures 7-10.

In Figure 11, we show the backtrack paths of the proposed drill sites relative to a fixed South America. Movement of South America in the absolute framework is very small compared to the oceanic plate motions, so these backtrack paths approximate real geography. Absolute poles of rotation for different time intervals are given in Table 3. In Figure 11, the absolute poles for South America were added to the absolute poles for each respective crustal plate to calculate the position of each drill site relative to South America.

Sites on the Nazca and Cocos plates backtrack paths for 0 to 19 Ma are based on the analysis of Pisias et al. (1995). Absolute poles of rotation for the Cocos plate (used for alternate Sites COC-2A, COC-3A, and COC-4A) were calculated using the pole of relative rotation between the Cocos and Pacific plates (36.823°N, 108.629°W, Ω = 2.09°/m.y. [DeMets et al., 1990]) and absolute poles for the Pacific plate (0- to 5-Ma pole = 61.6°N, 82.5°W, Ω = 0.97°/m.y. and for 5- to 20-Ma pole = 70.3°N, 74.4°W; Ω = 0.73°/m.y. [Cox and Engebretson, 1985]).

Absolute poles for the Nazca plate (used for Sites CAR-1C, CAR-2C, PAN-2A, NAZCA-10A, NAZCA-14A, NAZCA-16A, NAZCA-17A, SEPAC-9A, and SEPAC-10A) were calculated using relative motions between the Pacific and Nazca plates (pole = 55.58°N, 90.10°W; W = 1.42°/m.y.), and the absolute Pacific poles noted above. For the interval from 0 to 5 Ma, the resulting absolute pole for the Nazca plate is essentially identical to the pole given by Gripp and Gordon (1990). For the interval 19 to 42 Ma, Nazca plate sites were rotated using the absolute poles of Duncan and Hargraves (1984).

Absolute poles of rotation for the Antarctic plate (used for alternate Site SEPAC-5A) are from Cox and Engebretson (1985) and for South America are from Duncan and Richards (1991).

SCIENTIFIC OBJECTIVES

The primary scientific goal of paleoceanographers is to assess mechanisms of climate change as revealed by long-term changes in the ocean-climate system. In this regard, the role of the South Pacific is essentially unknown. The Leg 202 drilling experiment seeks to probe the climate system in three different, but compatible, ways. First, we seek to document the effect of tectonics on climate change, specifically the events associated with the opening of Drake Passage, the closing of the Panama Isthmus, and the uplift of the Andes Mountains. Second, we will document the Southern Hemisphere Eastern Boundary Current, eastern equatorial current, and subsurface water mass histories associated with the transition of climate regimes from one of polar warmth to one of glaciation in Antarctica, and eventually into the rhythmic Pleistocene ice ages of both the Northern and Southern Hemisphere. Third, we will seek a record of millennial-scale climate changes to assess the extent of rapid climate events as a test of two contrasting hypotheses. The first hypothesis is that rapid changes originate in the high North Atlantic Ocean and propagate elsewhere through the climate system, and the second hypothesis is that such changes originate in the low latitudes and propagate poleward.

Tectonic Impacts on Ocean Circulation and Climate

One of the most perplexing questions in climate is why global climate over the past 40 m.y. changed from very warm conditions (the "Greenhouse World") to conditions of unipolar (Southern Hemisphere) and later bipolar glaciation (the "Icehouse World"). Partial answers include plate tectonic processes, elevation and erosion of vast plateaus, opening and closing of oceanic gateways and changing concentrations of atmospheric greenhouse gases. The opening and closing of oceanic gateways are especially critical. The southeast Pacific Ocean is a key location to examine the response of the climate system to tectonic events, including the closure of the Isthmus of Panama, the opening of the Drake Passage, and the Neogene uplift of the Andes Mountains.

The opening of both the Australian-Antarctic gateway and the Drake Passage led to the development of the circumpolar current and consequently to a thermal isolation of Antarctica. This configuration is thought to be the ultimate cause for the initiation and continuation of Antarctic glaciation since about 35 Ma. This early cooling, including dramatic cooling of the deep sea (Kennett and Shackleton, 1976), and modified nutrient distributions within the global oceans (Brewster, 1980) are thought to reflect the slow drift of Australia away from Antarctica, which tended to isolate the southern continent (Kennett, 1974, 1977). However, considerable evidence exists for a much later opening of the Drake Passage, near 25 Ma (Barker and Burrell, 1977), which would contradict the hypothesis that the establishment of the Circum-Antarctic Current acted as final trigger for the Antarctic glaciation. Curiously, major expansion of ice in Antarctica is thought to have occurred (based on oxygen isotope and other data) near 15 Ma, 10 m.y. after the opening of Drake Passage. Thus, the climatic impact of Drake Passage opening, which created the Circumpolar Current, remains unknown. Numerical models predict a decrease of the Chile-Peru surface current and a distinct decrease in Antarctic deep and bottom water export to the north as water masses are entrained into a growing circumpolar circulation (Mikolajewicz et al., 1993). Site SEPAC-9A from the Chile Basin and Sites NAZCA-10A and 17A will provide an excellent opportunity to examine the timing and impact of the Drake Passage opening on the proposed changes in ocean circulation.

The Neogene tectonic closure of the Central American Isthmus from 13.0 to 2.7 Ma (Duque-Caro, 1990; Collins et al., 1996) resulted from the subduction of the Pacific, Cocos, and Nazca plates beneath the North and South American plates and, later, the Caribbean plate. The closure has always been an attractive candidate for the ultimate cause of the Pliocene intensification of the Northern Hemisphere glaciation since ~3.1 Ma (Mikolajewicz and Crowley, 1997). Closure-induced changes in global thermohaline circulation have been invoked to be the cause either for the onset (Berggren and Hollister, 1974) or for the delay (Berger and Wefer, 1996) or for setting the preconditions of the Northern Hemisphere glaciation (Haug and Tiedemann, 1998; Driscoll and Haug, 1998).

While the link between the isthmus closure and the Northern Hemisphere glaciation is still a matter of debate, recent studies clearly identify a close link between the formation of the Panama Isthmus and major oceanographic changes that occurred between 4.6 and 4.2 Ma, when the Panamanian sill shoaled to a water depth of <100 m (Haug and Tiedemann, 1998). The chain of evidence suggests the development of the modern Pacific-Atlantic salinity contrast of ~1‰ (Haug et al., 2001), a reorganization of the equatorial Pacific surface current system, the intensification of upper North Atlantic Deep Water formation, and the development of the modern chemical Atlantic-Pacific asymmetry, which is reflected in a strong increase in Caribbean/Atlantic carbonate preservation and a remaining strong carbonate dissolution in the Pacific (Haug and Tiedemann, 1998; Haug et al., 2001; Farrell et al., 1995; Cannariato and Ravelo, 1997). This major salinity contrast between ocean basins, driven in part by net freshwater transport as vapor across the Panama Isthmus, is likely responsible for maintaining the global thermohaline "conveyor belt" circulation, which is dominated by North Atlantic Deep Water (Gordon, 1986; Broecker, 1991). Changes in the equatorial surface current system will be monitored by sites from the Cocos and Carnegie Ridges. Changes in intermediate water chemistry that result from a restricted exchange of water masses through the Panamanian gateway because of late Miocene to early Pliocene shoaling of the sill depth will be registered by a comparison of sites from the Caribbean and Leg 202 (CAR-1C and NAZCA-10A).

The uplift of the Andes is expected to have caused significant changes in atmospheric circulation, wind-driven oceanic surface circulation, and hence, productivity. Marked changes in the uplift history of the Andes were detected during Leg 154 (Ceara Rise) by drilling the Atlantic side of South America. The increase in the Amazon River supply of terrigenous sediments and its change in clay mineralogy indicate major uplift phases from 12 to 8 Ma and since ~4.6 Ma (Curry, Shackleton, Richter, et al., 1995). This is consistent with paleobotanical reconstructions from the Central and Columbian Andes Mountains, assuming major phases of uplift since 10 Ma (Gregory-Wodzicki, 2000) and 4.6 Ma (Hooghiemstra and Ran, 1994; van der Hammen et al., 1973). The early Pliocene phase is paralleled by the subduction of the Cocos Ridge at ~5 Ma, which formed during the passage of the Cocos plate over the Galapagos hotspot, and dramatically elevated the Central American volcanic arc and led to the final phase of the closure of the Isthmus of Panama (Dengo, 1985; Hoernle et al., pers. comm., 2001). If this hypothesis is true, analogous changes in clay mineralogy are expected in the hemipelagic sediment records of Leg 202. Unfortunately, the land record can not be used to assess the details of Neogene water mass changes that respond to mountain uplift, as the land record of marine sediments contains major hiatuses, for example, in

Chile between 10 and 3.5 Ma (Martinez-Pardo, 1990). The hemipelagic sites contain significant terrigenous clay and will provide opportunities for understanding climatic and tectonic evolution on land as well as changes in marine environments.

Orbital and Polar Ice Sheet Impacts on Ocean Circulation and Climate.
Sites to be drilled during Leg 202 will provide an extraordinary opportunity to examine the details of regional climate responses to the onset and amplification of Pleistocene ice age cycles at orbital scales over the last 5 Ma. Evidence from the Southern Ocean (Imbrie et al., 1993) and from the equatorial Pacific Ocean (Pisias and Mix, 1997; Lea et al., 2000) suggest that near-surface changes in these areas precede those at high northern latitudes. Thus, climate changes here do not passively respond to Northern Hemisphere glaciation but could be part of the chain of responses that lead to Northern Hemisphere glaciation. Especially important for Leg 202 will be to assess the linkages between changes observed at higher southern latitudes (e.g., SEPAC-9A, 13A, and 14A) with those along the equator (CAR-1C, CAR-2C, and PAN-2). Site NAZCA-17A will provide a useful monitor of the advective link between the high and low latitudes, by monitoring the strength of the cool Humboldt Current.

Waters advected off the eastern boundary have a profound influence on the equatorial Pacific Ocean and have a significant role in maintaining the equatorial cold tongue (Bryden and Brady, 1985; Liu and Huang, 2000). The Peru-Chile Current and its extension into the equatorial Pacific Ocean are thought to have been stronger than at present during the last glacial maximum (LGM) (CLIMAP, 1976; Pisias and Mix, 1997; Mix et al., 1999b; Feldberg and Mix, in press). This current may have acted as a conduit for cold near-surface water from high latitudes to enter the cool tongue of the South Equatorial Current (SEC). Assessing the relative roles of advection of cold low-nutrient surface waters vs. upwelling of higher-nutrient subsurface waters into the equatorial Pacific Ocean are important because upwelled waters create very high surface-water pCO_2. Advected surface water would be a weaker CO_2 source. At present, the equatorial Pacific Ocean is a large net source of CO_2 to the atmosphere (Tans et al., 1990), but the magnitude of this source has changed through time (Jasper et al., 1994), perhaps with global consequences. Understanding both the history of water masses and biological production (Mix, 1989) will be important in assessing the role of the eastern equatorial Pacific Ocean in the long-term balance of atmospheric CO_2.

Significant changes in the SEC were inferred from ODP Site 846 (3°S, 91°W; 3307 m depth), which was drilled during Leg 138 to examine the interaction of eastern boundary waters with the equatorial currents. Quaternary planktonic foraminifers found here (Le et al., 1995) vary between a warm subtropical fauna (*Globerinita. glutinata* and *Globigerinoides sacculifer*), a cool-water fauna advected off the Peru margin (*Globigerina bulloides*), and higher-latitude fauna (*Globorotalia inflata*) that reflect northward advection in the Eastern Boundary Current. The obvious next step is to examine relationships between the tropical Pacific Ocean and the eastern boundary of the southeast Pacific Ocean in a latitudinal transect within the Peru-Chile Current, with targets in late Pleistocene ice ages and in older preglacial times.

Another climatic puzzle that has long interested paleoceanographers is the apparent regional stability of subtropical climates during the LGM (CLIMAP, 1981) and the apparent differences in the timing and amplitude of climate changes at the poles relative to those observed near the equator (e.g., Imbrie et al., 1989). These results have been questioned, as some data and models suggest that climate changes at the poles (especially the expansion of polar ice sheets and sea ice) and changes in greenhouse gases should influence global climate (Pinot et al., 1999). A legitimate concern regarding the low amplitude of change in the CLIMAP study of the LGM was that many samples from the subtropics had very low sedimentation rates, to the point that bioturbation could suppress real changes by mixing together glacial and interglacial fossil assemblages. Leg 202 may be able to address the controversy of the stable subtropics in a different way, by examining the response of the Southern Hemisphere subtropics to long-term growth of glaciation in Antarctica (with major expansion of ice near 15 Ma) and again to expansion of global glaciation within the past ~5 Ma. Sites SEPAC-9A, NAZCA-10A, and NAZCA-17A are especially well suited to this study, as they will span paleolatitudes from ~17° to 41°S over a broad time range.

Within Pleistocene time, the origin of the large 100-k.y. climate cycle at ~1 Ma remains puzzling. A number of mechanisms have been proposed, including a threshold response of high-latitude glaciers to gradual long-term cooling associated with uplift of mountain ranges (Ruddiman and Raymo, 1988) or reduction of greenhouse gases (Maasch and Saltzman, 1990), erosion of soft sediment below Northern Hemisphere glaciers to expose bedrock, allowing larger glaciers to grow by increasing basal friction (Clark and Pollard, 1998), atmospheric loading of cosmic dust to trigger a response to rhythmic changes in the plane of Earth's orbit (Muller and MacDonald, 1997), and long-term cooling of the deep sea at polar outcrops, which influenced sea-ice distributions (Gildor and Tziperman, 2001). A 100-k.y. cycle of climate may also originate independently of polar climate changes via a nonlinear response of tropical climate systems to orbital changes in seasonal insolation (Crowley et al., 1992). Evidence exists for rhythmic 100-k.y. cycles of sedimentation in the eastern tropical Pacific Ocean, which if climatically significant could have provided a "template" for a climate cycle that was later picked up by the global ice sheets (Mix et al., 1995). A range of evidence suggests that tropical climate changes at orbital scales preceded those of the Northern Hemisphere ice sheets and must vary independently of the high northern latitudes (Imbrie et al., 1989, McIntyre et al., 1989; Pisias and Mix, 1997; Harris and Mix, 1999; Lea et al., 2000).

Millennial-Scale Climate Changes—Polar or Tropical Causes?

A primary initiative for ODP is to understand the causes and consequences of millennial-scale climate change. Such changes are well documented in rapidly accumulating North Atlantic Ocean sediments (e.g., Labeyrie and Elliot, 1999; Clark et al., 1999). This has led to hypotheses that millennial-scale changes are driven either by instabilities in Northern Hemisphere ice sheets that surround the North Atlantic Ocean (MacAyeal, 1993) or by oscillations in the formation of North Atlantic Deep Water (Broecker et al., 1990) or, in some cases, perhaps to rhythmic solar forcing (Bond et al., 1997).

Similar millennial-scale climatic oscillations have been detected in the northeast Pacific Ocean (e.g., Hendy and Kennett, 1999, 2000), suggesting the transmission of rapid climate change events from their North Atlantic origins into the North Pacific Ocean (Mikolajewicz et al., 1997). An alternative hypothesis (though perhaps not mutually exclusive) is that rapid climate oscillations may emanate from the tropics, where they originate as an unstable response to insolation (McIntyre and Molfino, 1996), perhaps as oscillations in the frequency of El Niño Southern Oscillation (ENSO) events of the eastern tropical Pacific Ocean (Cane and Clement, 1999). This hypothesis is plausible given lake and ice core records from South America that suggest long-term changes in the mean state of ENSO events (Rodbell et al., 1999; Thompson et al., 1998), glacial-interglacial sea-surface temperature changes that mimic spatial patterns of change associated with modern La Niña events (Pisias and Mix, 1997; Mix et al., 1999b; Beaufort et al., 2001), and model results suggesting sensitivity of long-term average oceanic condition to changes in El Niño frequency, forced by orbital insolation (Clement et al., 1999). On an interannual scale, Liu and Huang (2000) argue based on modern heat budgets that warming in the region over the past 50 yr is related to reduction of the wind-driven advection of cool water off the eastern boundary and that such effects that dominate the eastern tropical Pacific extend even to the western Pacific Ocean and, perhaps, elsewhere. If this tropical hypothesis is true, we expect that millennial-scale climate events will be clearly recorded in sites with high sedimentation rates from the eastern equatorial Pacific Ocean, particularly near the Galapagos region, which is the area to be sampled at Site PAN-2A.

Denitrification associated with low-oxygen water masses in the eastern Pacific Ocean produces N_2O, consuming nutrients, presenting a net source to the atmosphere. As this region is the largest center of denitrification in the global ocean it is likely to dominate the global budget. This may open a unique opportunity in high-resolution paleoclimatology. If variations in the strength of the oxygen minimum (recorded by geochemical tracers and benthic faunal assemblages) (e.g., Phleger and Soutar, 1973; Oberhänsli et al., 1990) and denitrification (detected via nitrogen isotope analyses of organic matter) (Ganeshram et al., 1995) in the eastern tropical Pacific Ocean prove to be responsible for a substantial portion of global variations in N_2O observed in polar ice cores, the rich archives of paleoclimatic variations recorded in these two areas may be synchronized at high resolution.

Recent data, especially from the northeast Pacific Ocean (Behl and Kennett, 1996; Lund and Mix, 1998; Mix et al., 1999a) affirms the importance of understanding Pacific deep and intermediate water circulation on millennial timescales. Broecker (1998) points to the existence of a "bipolar seesaw" effect, in which millennial-scale changes in Antarctic temperature are out of phase with (leading) Northern Hemisphere events. This inference is buttressed by data from the Southern Ocean (Charles et al., 1996) and by comparison of ice-core $\delta^{18}O$ or D/H data from both hemispheres, synchronized with the methane record (Blunier et al., 1998). Because the patterns of change are significantly different in the Northern and Southern Hemispheres, we can use the pattern of ventilation events on the millennial scale as a "fingerprint" of their source.

ODP Site 893 from the Santa Barbara Basin provides compelling evidence of millennial-scale events of enriched oxygen content (i.e, unvarved sediments containing oxic benthic foraminiferal assemblages) that are approximately correlated with cold events in the North Atlantic Ocean (Kennett and Ingram, 1995; Behl and Kennett, 1996; Cannariato et al., 1999). The process driving such changes, however, remains uncertain. Variations in the bottom waters of the Santa Barbara Basin may reflect ventilation of intermediate water originating either in the North or South Pacific Ocean, changes in local productivity and its effect on oxygen content within the basin, or changes in regional productivity of the North Pacific Ocean that change the character of the oxygen minimum zone. Ventilation from the north is certainly possible and would be consistent with modeling studies that link NPIW ventilation to North Atlantic cooling during the Younger Dryas (Mikolajewicz et al., 1997). Other sites along the California margin and the Gulf of California show millennial-scale variations in intermediate and surface water properties, but limitations in dating so far preclude a definitive link to Younger Dryas cooling (van Geen et al., 1996; Keigwin and Jones, 1990).

Radiocarbon-dated evidence of organic carbon at ODP Site 1019 (980 m water depth off Northern California) indicates that regional productivity effects could contribute to variations in the oxygen minimum zone off California (Mix et al., 1999a). At this site, benthic foraminiferal $\delta^{13}C$ values suggest ventilation of intermediate water masses during the transition from warm (Bølling-Allerød) to cold (Younger Dryas) climate events (i.e., intermediate water ventilation leads to cooling). This apparent phasing between surface temperature and benthic $\delta^{13}C$ values within the same samples is important because it suggests that the ventilation event at intermediate depths of the North Pacific Ocean may lead the Younger Dryas cooling. Thus, evidence from ODP Site 1019 suggests that it is unlikely that intermediate water ventilation responds directly to North Atlantic cooling during the Younger Dryas event, as predicted for NPIW by some climate models (Mikolajewicz et al., 1997). The event with high benthic $\delta^{13}C$ values is from ~14.5 to 13 ka, similar to the timing of the Antarctic Cold Reversal as recorded in the Byrd ice core of Antarctica (Blunier et al., 1997). Flushing with AAIW, consistent with the LGM model circulation of Campin et al. (1999) might explain this event.

Leg 202 sites will contribute to our understanding of millennial-scale climate changes by providing records of change in high-sedimentation rate sites within the equatorial cold "tongue" (Site PAN-2A) and off central Chile (Sites SEPAC-13A, SEPAC-14A, and, if drilled, alternate Site SEPAC-19A). Site PAN-2A is ideally located to assess rapid variations in equatorial upwelling, perhaps related to long-term stability of ENSO events. The SEPAC sites are particularly well located for assessing variations in the strength of AAIW through time. Sedimentological evidence suggests that rapid climate changes are recorded off central Chile (Lamy et al., 1999) and are supported by evidence for millennial-scale oscillations in Andean glaciers (Lowell et al., 1995).

Ancillary Studies

Leg 202 may provide materials for several studies not closely linked to its primary paleoceanographic objectives.

(a) Basement ages at Site SEPAC-9A are not well defined because a significant number of small fracture zones exist in the area. Basal sediment ages will provide new constraints on regional tectonics.
(b) Basal sediment ages on Nazca Ridge will improve knowledge of this fossil hotspot track.
(c) Site survey data for Leg 202 revealed bathymetric evidence for large-scale slumping of sediments on the south flank of Carnegie Ridge. A possible sliding layer for such slumps are the organic-rich sediments deposited at ~10 Ma in a broad region of the eastern equatorial Pacific Ocean (Kemp et al., 1995). We expect to sample these features during Leg 202 at Site CAR-2C and will seek structural evidence that might constrain the timing and processes responsible for large-scale downslope movements of sediments in the region.

PROPOSED DRILLING SITES

Tables 1 and 2 list approved primary and alternate sites, respectively.

Chile Margin (Primary Sites SEPAC-13B, SEPAC-14A; Alternate Site SEPAC-19A)

These sites form a depth transect to monitor AAIW (with higher oxygen content than overlying waters of the GU and deeper PCW). Sedimentation rates are expected to be high (>20 cm/k.y.) and, thus, these sites will provide a high-resolution record of climate change off central Chile. Sites SEPAC-13A and SEPAC-14A are within a highly productive coastal upwelling area near Concepcion. To the south, Site SEPAC-19A lies in the transition zone between the subtropical and subpolar gyres and thus may help to monitor latitudinal translations of the northern boundary of the westerly wind belt on millennial scales.

Chile Basin (Primary Site SEPAC-9A; Alternate Site SEPAC-10A)

The drill sites in the Chile Basin appear to be on relatively old oceanic crust (Cande and Haxby, 1991) and will provide records as old as 50 Ma (Tables 1, 2), suitable for testing the subtropical oceanographic effects of opening Drake Passage, as well as for reconstruction of younger events.

Although sedimentation rates are probably low (~1-2 cm/k.y.) and carbonate preservation poor, these sites provide an important location to monitor CPDW, if benthic foraminifers are consistently present.

Chile Rise (Alternate Site SEPAC-5A)

The Chile Rise provides a good location to monitor the depth and chemistry of CPDW at relatively low latitudes. At its shallowest, this active spreading ridge is young and sediment cover is thin. Previous ODP drilling on the eastern Chile Rise area during Leg 141 concentrated on tectonic objectives in the zone of deformation where the Chile Rise interacts with the subduction zone. Excellent information on regional magnetic anomalies and tectonics that led to Leg 141 (Herron et al., 1981; Cande and Leslie, 1986; Cande et al., 1987), however, provide good control on basement ages of the sites proposed here. Alternate Site SEPAC-5A is south of the Chile Rise axis on the Antarctic plate. Because the crust here spreads westward relative to the eastward propagating ridge axis, this site will maintain a relatively steady geographic position near the South American margin throughout its history. Site SEPAC-5A is considered to be an alternate site for Leg 202 because of the significant transit time to the site, the relatively young crust that limits the length of record, and because the cores taken during the site survey cruise are barren of microfossils in many intervals.

Nazca Ridge (Primary Sites NAZCA-10A, 17A; Alternate Sites NAZCA-14A, 16A)

The Nazca Ridge provides sites to monitor a latitude band where the near-surface cool tongue of the Peru-Chile Current is well developed. This ancient aseismic ridge, a fossil hotspot track, is sediment covered to its shallowest reaches. Basement ages are estimated based on the magnetic anomalies of the surrounding oceanic crust (Cande and Haxby, 1991). If we assume that the Nazca Ridge was formed at the Easter Island hotspot, then the age difference between the basement of the ridge and adjoining plate may only be a few million years. If so, the drill sites on the Nazca Ridge have the potential of providing pelagic records spanning the entire Neogene and possibly as old as the late Oligocene time. Site NAZCA-10 will help to monitor the boundary between PCW and AAIW.

Cocos and Carnegie Ridges (Primary Sites CAR-1C, CAR-2C, PAN-2A; Alternate Sites COC-2A, COC-3A, COC-4A)

In the regions proposed for coring, the Cocos and Carnegie Ridges are fossil traces of volcanism at the Galapagos hotspot split by seafloor spreading at the Galapagos Rift. Shallow sites of the ridge crests appear to be drowned volcanic seamount tops. Both ridges are heavily sedimented. Sediments here are typically comprised of nannofossil-foraminifer ooze, with diatoms and radiolarians. In the site documentation, basement ages are based on the tectonic reconstructions of Hey et al., (1977) and Lonsdale and Klitgord (1978) extrapolated from regional magnetic anomalies in normal oceanic crust. The age of basement sampled at DSDP Site 158, cored on the north flank of Cocos Ridge, is ~12 to 14 Ma. The ridges, although basically aseismic, retain some seismicity associated with interaction of the ridges with subduction zones off Ecuador (Carnegie Ridge) and Costa Rica (Cocos Ridge). To the south of Cocos Ridge and west of Carnegie Ridge, the Galapagos Islands are volcanically active. Near the equator, the Cocos and Carnegie Ridges, which form the boundaries of the Panama Basin, provide an excellent opportunity for a depth transect from <1000 to ~4000 m. Water chemistry at the seafloor here reflects the southward flow of high-nutrient, low-oxygen North Pacific water, but may also respond to high equatorial and eastern boundary productivity. Sites CAR-1C and CAR-2C will monitor intensity of the equatorial Pacific cold tongue at its eastern boundary over the last ~15 m.y. Site PAN-2A will provide a shorter record, perhaps 5 m.y., but at relatively high sedimentation rates (10-15 cm/k.y.) suitable for analysis of millennial-scale climate changes. Sites on the Cocos Rise (Alternate Sites COC-2A, 3A, and 4A) underlie the low-salinity surface ocean layer west of the Panama Isthmus and thus help monitor long-term changes in cross-isthmus transport of fresh water vapor across the Panama Isthmus.

SURVEY STRATEGY

All sites included in this prospectus were surveyed and approved for coring by the Pollution Prevention and Safety Panel (PPSP). However, no crossing seismic line is available at Site SEPAC-13B. To optimize site locations, a short survey (~7 hr) will be conducted over proposed Sites SEPAC-13B and SEPAC-14A using the *JOIDES Resolution's* 80 in^3 air gun on approach to the sites. Alternate Site SEPAC-19A has no crossing line, and if it is drilled a short (~2 hr) survey using the *JOIDES Resolution's* 3.5-kHz profiler will be executed to optimize the site location within the basin.

DRILLING STRATEGY

All sites will be triple-cored with the advanced piston corer (APC) to refusal. APC refusal depth is estimated at 150-250 meters below seafloor (mbsf). The mudline should be recovered in at least two holes at each site. Additional short APC holes may be drilled if this is required to achieve complete stratigraphic coverage (i.e., to eliminate all coring gaps and disturbed intervals in a composite section) in the APC interval. If the target depth is greater than the APC refusal depth, one hole (usually hole B) will be deepened with the extended core barrel (XCB). A second XCB interval may be cored at some sites if time becomes available or if the results warrant such an effort.
Based on coring and logging time estimates, eight high-priority sites can be cored in the time available (Table 1). The sequence of drilling will essentially follow the south-north track of the ship from Valparaiso to Balboa. It is expected that at least one more high-priority site (SEPAC-19A and/or COC-3A) can be drilled using modest time gains, including an early departure and faster transits and coring. Depending on the coring results and the time available after completion of the southern area primary sites (SEPAC-14A, 13B, and 9A), contingency Site SEPAC-19A may be cored before departing north. If time is available later in the cruise, Site COC-3A is expected to be the first contingency site to be cored in the northern area.

If further time becomes available during the leg, the contingency plans include coring at second priority (alternate) sites (Table 2) and/or coring additional XCB intervals in an attempt to extend the composite section below the APC interval.

LOGGING PLAN

Under the primary operations plan, logging will be carried out at each of the five sites with penetration of ≥300 mbsf (Table 1). Three tool strings will be run at the logged sites: the triple combination (triple combo) (resistivity, density, porosity, and natural gamma logs); the Formation MicroScanner (FMS)/sonic (resistivity image, acoustic velocity, and natural gamma logs); and the geologic magnetic tool (GHMT) (magnetic field, susceptibility, and natural gamma logs). In addition, the third-party Lamont multisensor gamma tool (MGT) with about four times the vertical resolution of standard natural gamma tools will also be deployed on the triple combo string.

Coring seeks to answer questions about rapid and tectonic-scale climate changes and their link to regional oceanographic currents and Southern Hemisphere wind patterns. The expected changes will drive lithologic variability in both the biogenic components as well as the amount and type of terrigenous material that can be well documented by standard logging techniques. The density, porosity, and resistivity logs will provide continuous records of climate related changes in sediment lithology (e.g., percent $CaCO_3$) where core recovery may not be 100%. With higher resolution, the FMS and MGT will provide continuous records of lithologic variability and terrigenous input on orbital to suborbital timescales. The FMS also allows imaging of fine-scale bedding in poorly recovered intervals.

The recovery of continuous sediment sections is a critical component to the success of the leg. Recent paleoceanographic legs with similar high-resolution goals have demonstrated the importance of core-log integration in developing a reliable composite section. The core-log integration program Sagan will be used to correlate downhole natural gamma ray, density, and magnetic susceptibility logs to their counterpart core measurements to provide more precise depth matching of cored sections and real-time assessment of the accuracy of the shipboard splice.

For more detailed information on any particular tool or its application, please see the Borehole Research Group (BRG) website at http://www.ldeo.columbia.edu/BRG/.

SHIPBOARD LABORATORY OPERATIONS

Core Logging and Archiving Strategy

Multiple hole coring aims to fill coring gaps from one hole with recovered sequences from another hole. Ideally, the stratigraphic correlator will able to tell the driller (or core technician) at what depth the drill string should be placed for shooting the third hole, based on the correlation of the top cores from the first two holes. The multisensor track (MST) core logging often lags many hours behind at that point, and full MST logging runs are too slow to provide the quick feedback required to guide coring.

To address this issue, we tentatively plan to install a specialized (non-ODP) track with a magnetic susceptibility loop to perform quick "scratch" measurements for the sole purpose of rapidly determining the required coring interval. We will attempt to run this specialized track immediately after core sections are cut on the catwalk, at a rate of ~1 min per core section (under the guidance of the stratigraphic correlators).

An important part of the shipboard measurements at each site will be the near-real time construction of a composite depth section from multiple holes (for purposes of later sampling) and an alternate spliced section as complete as possible (for purposes of ODP archiving) for the multi-hole intervals at all sites. Two dedicated stratigraphic correlators will operate the whole-core MST, retrieve the relevant data from the database, and correlate cores from multiple holes by vertical whole-core depth shifting. The MST sampling program will be set to optimize measurement time (within constraints of adequate data quality and depth resolution) for the overall time available. In typical operations, about 60-90 min will be available to process one core (~10 m), which will also set the core processing rate for all other laboratory stations.

After MST measurements are completed, the cores will be split. Working halves will be transferred to the paleomagnetics laboratory, followed by sampling noted below. Archive halves will be imaged using the new ODP core imaging system that will be deployed and tested during Leg 198. These high-resolution R-G-B image data may not yet be fully integrated into the *JOIDES Resolution's* database system during Leg 202 and data transfer protocols may have to be created ad hoc. Following digital imaging, routine color reflectance measurements will be taken with the automated Minolta CM2002 after the cores are split and can be used to refine the hole-to-hole correlation. The imaging and color reflectance tracks will be operated by the sedimentology group. Under ideal core processing conditions, these core logging data should be available ~2 hr after the full core measurements. Archival photography will be completed using standard ODP film photography.

SAMPLING STRATEGY

Sample Requests

It is the cruise participants' responsibility to read and understand the ODP Sample Distribution, Data Distribution, and Publications Policy, which can be found at http://www-odp.tamu.edu/publications/policy.html

Sample requests can be submitted by shipboard and shore-based participants at any time. Participants are asked to submit a request no later than 3 months precruise. Requests received precruise may have precedence over competing requests made during the cruise. All precruise requests will be posted on the ODP web page and the URL will be made available to the Leg 202 participants only. The Sample Allocation Committee (SAC; co-chiefs, staff scientist, and ODP curator) encourages participants to contact each other and coordinate sample requests and proposed work before the cruise to minimize this effort during the precious time available during the cruise. The draft sampling plan will be prepared at the beginning of the cruise by the scientific party, under the leadership of the SAC, and refined during the cruise based on the actual coring results. The final sampling plan will be highly integrated, ensuring that essential work will be completed on all intervals and that duplication will be avoided.

Shipboard Sampling

Samples for routine shipboard analyses of ephemeral properties and for measurements essential to safety monitoring and initial shipboard interpretations will be taken during the cruise by the responsible laboratory representatives.

Catwalk Samples:

- Vacutainer samples of free gas,
- Headspace samples for organic geochemistry,
- Interstitial water samples for inorganic geochemistry, and
- Core catcher samples for biostratigraphic analyses.

Working-Half Core Samples:

- 10-cm^3 samples for moisture and density determination (~1/section),
- 6-cm^3 samples for carbonate concentration (coulometry) (~1/section), and
- 2-cm^3 samples for x-ray diffraction (XRD) and/or inductively coupled plasma-mass spectrometery (ICP-MS) as needed.

In addition, individual sample requests for intervals recovered in only one hole, such as some of the deeper XCB intervals, will be sampled on the ship with the approval of the SAC. All shipboard participants will participate in the sampling effort, regardless of their personal sampling plan.

Sampling the Stratigraphic Splice Sections (Postcruise)

Whenever possible, samples for postcruise research will be taken from the splice constructed by hole-to-hole correlation of cores during the cruise. Such sampling will maximize integration and impact of scientific results. Because it takes a few days to complete the composite depth section and splice (and more time to prepare adequate sampling templates), such sampling will not be possible during the cruise. The cores will be stored away and the laboratory busy with the cores from a subsequent site. Sampling of the composite depth sections is therefore deferred to one or two postcruise sampling party(ies) ~3-5 months postcruise in College Station, Texas.

REFERENCES

Barker, P.F., and Burrell, J., 1977. The opening of Drake Passage. *Mar. Geol.,* 25:15-34.

Beaufort, L., Gariel-Thoron, T., Mix, A.C., Pisias, N.G., 2001. ENSO-like forcing on oceanic primary production during the late Pleistocene. *Science,* 293:2440-2444.

Behl, R.J., and Kennett, J.P., 1996. Brief interstadial events in the Santa Barbara Basin, NE Pacific, during the past 60 kyr. *Nature,* 379:243-246

Berger, W.H., Lange, C.B., and Weinheimer, A., 1997. Silica depletion of the thermocline in the eastern North Pacific during glacial conditions: clues from Ocean Drilling Program Site 893, Santa Barbara Basin, California. *Geology,* 25:619-622.

Berger,W.H., and Wefer, G., 1996. Expeditions into the past: paleoceanographic studies in the South Atlantic. *In* Wefer, G., Berger, W.H., Siedler, G., and Webb, D.J. (Eds.), *The South Atlantic: Present and Past Circulation:* Berlin (Springer-Verlag), 363-410.

Berggren, W.A., and Hollister, C.D., 1974. Paleogeography, paleobiogeography, and the history of circulation of the Atlantic Ocean. *In* Hay, W.W. (Ed.), *Studies in Paleoceanography.* Soc. Econ. Paleontol. Mineral. Spec. Publ., 20:126-186.

Bloomer, S.F., Mayer, L.A., and Moore, T.C., 1995. Seismic stratigraphy of the eastern equatorial Pacific Ocean: paleoceanographic implications. *In* Pisias, N.G., Mayer, L., Janecek, T., Palmer-Julson, A., van Andel, T.H. (Eds.), *Proc. ODP, Sci. Results* 138: College Station, TX (Ocean Drilling Program), 537-553.

Blunier, T., Chappellaz, J., Schwander, J., Dällenbach, A., Stauffer, B., Stocker, T.F., Raynaud, D., Jouzel, J., Clausen, H.B., Hammer, C.U., and Johnsen, S.J., 1998. Asynchrony of Antarctic and Greenland climate change during the last glacial period. *Nature*, 394:739-743.

Blunier, T., Schwander, J., Stauffer, B., Stocker, T., Dällenbach, A., Indermühle, A., Tschumi, J., Chappellaz, J., Raynaud, D., Barnola, J.M., 1997. Timing of the Antarctic Cold Reversal and the atmospheric CO_2 increase with respect to the Younger Dryas event. *Geophys. Res. Lett.*, 24:2683-2686.

Bond, G., Showers, W., Cheseby, M., Lotti, R., Almasi, P., deMenocal, P., Priore, P., Cullen, H., Hajda, I., and Bonani, G., 1997. A pervasive millennial-scale cycle in North Atlantic Holocene and Glacial climates. *Science,* 278:1257-1266.

Brewster, N.A., 1980. Cenozoic biogenic silica sedimentation in the Antarctic Ocean. *Geol. Soc. Amer. Bull.,* 91:337-347.

Broecker, W.S., 1991. The great ocean conveyor. *Oceanography,* 4:79-89.

Broecker, W.S., 1998. Paleocean circulation during the last deglaciation: A bipolar seesaw? *Paleoceanography,* 13:119-121.

Broecker, W.S., Bond, G., Klas, M., Bonani, G., and Wolfli, W., 1990. A salt oscillator in the glacial Atlantic? 1. The concept. *Paleoceanography,* 5:469-478.

Bryden, H.L., and Brady, E.C., 1985. Diagnostic model of the three-dimensional circulation in the upper Equatorial Pacific Ocean. *J. Phys. Oceanogr.,* 15:1255-1273.

Campin, J.-M., Fichefet, T., and Duplessy, J.-C., 1999. Problems with using radiocarbon to infer ocean ventilation rates for past and present climates. *Earth Planet. Sci. Lett.,* 165:17-24.

Cande, S.C., and Haxby, W.F., 1991. Eocene propagating rifts in the Southwest Pacific and their conjugate features on the Nazca plate. *J. Geophys. Res.*, 96(B12):19609-19622.

Cande, S.C., and Kent, D.V., 1995. Revised calibration of the geomagnetic polarity timescale for the late Cretaceous and Cenozoic. *J. Geophys. Res.*, 100:6093-6095.

Cande, S.C., and Leslie, R.B., 1986. Late Cenozoic tectonics of the southern Chile Trench. *J. Geophys. Res.,* 91(B1):471-496.

Cande, S.C., Leslie, R.B., Parra, J.C., and Hobart, M., 1987. Interaction between the Chile Ridge and Chile Trench: geophysical and geothermal evidence. *J. Geophys. Res.* 92(B1):495-520.

Cane, M., and Clement, A.C., 1999. A role for the tropical Pacific coupled ocean-atmosphere system on Milankovitch and millennial timescales, Part II: global impacts. *In* Clark, P., Webb, R., Keigwin, L., (Eds.), *Mechanisms of Global Climate Change at Millennial Scales:* Geophys. Monogr., Am. Geophys. Union, 112:373-383.

Cannariato, K.G., Kennett, J.P., Behl, R.J., 1999. Biotic response to late Quaternary rapid switches in Santa Barbara Basin: ecological and evolutionary implications. *Geology*, 27:63-66.

Cannariato, K.G., and Ravelo, A.C., 1997. Pliocene-Pleistocene evolution of the eastern Pacific surface water circulation and thermocline depth. *Paleoceanography*, 12:805–820.

Charles, C.D., Lynch-Stieglitz, J., Ninnemann, U.S., and Fairbanks, R.G., 1996. Climate connections between the hemisphere revealed by deep sea sediment core/ice core correlations. *Earth Planet. Sci. Lett.,* 142:19-27.

Christie, D.M., Duncan, R.A., McBirney, A.R., Richards, M.A., White, W.M., Harp, K.S., and Fox, C.G., 1992. Drowned islands downstream from the Galapagos hotspot imply extended speciation times. *Nature*, 355:246-248.

Clark, P.U., and Pollard, D., 1998. Origin of the middle Pleistocene transition by ice sheet erosion of regolith. *Paleoceanography* 13:1-9.

Clark, P.U., Webb, R.S., Keigwin, L.D. (Eds.), 1999. *Mechanisms of Global Climate Change at Millennial Time Scales*, Geophys. Monogr., Am. Geophys. Union, 112.

Clement, A.C., Seager, R., and Cane., M.A., 1999. Orbital controls on the El Niño/Southern Oscillation and the tropical climate. *Paleoceanography,* 14:441-456.

CLIMAP Project Members, 1976. The surface of the ice age Earth. *Science,* 191:1131-1137.

CLIMAP Project Members, 1981. Seasonal reconstruction of the Earth's surface at the last glacial maximum. *Geol. Soc. Amer., Map and Chart Ser.,* MC36.

Codispoti, L.A., and Christensen, J.P., 1985. Nitrification, denitrification, and nitrous oxide cycling in the eastern tropical South Pacific Ocean. *Mar. Chem.,* 16:277-300.

Collins, L.S., Coates, A.G., Berggren, W.A., Aubry, M.-P., and Zhang, J., 1996. The late Miocene Panama Isthmian Strait. *Geology,* 24:687-690.

Cox, A., and Engebretson, D., 1985. Changes in motion of Pacific plate at 5 Myr BP. *Nature*, 313:472-474.

Crowley, T.J., Kim, K.-Y., Mengel, J.G., and Short, D.A., 1992. Modeling 100,000-year climate fluctuations in pre-Pleistocene time series. *Science,* 255:705-707.

Curry, W.B., Shackleton, N.J., Richter, C., et al., 1995. *Proc. ODP, Init. Repts.*, 154: College Station, TX (Ocean Drilling Program).

DeMets, C., Gordon, R.G., Argus, D.F., and Stein, S., 1990. Current plate motions. *Geophys. J. Int.,* 101:425-478.

Dengo, G., 1985. Tectonic setting for the Pacific margin from southern Mexico to northwestern Columbia. *In* Nairn, A.E., Stehli, F.G., and Uyeda, S. (Eds.), *The Pacific Ocean: The Ocean Basins And Margins, 7A*, New York (Plenum Press), 123-180.

Driscoll, N.W., and Haug, G.H., 1998. A short circuit in thermohaline circulation: a cause for northern hemisphere glaciation? *Science,* 282:436-438.

Duncan, R.A., and Hargraves, R.B., 1984. Plate tectonic evolution of the Caribbean region in the mantle reference frame. *In* Bonini, W.E., Hargraves, R.B., Shagam, R. (Eds), *The Caribbean-South American Plate Boundary and Regional Tectonics.* Mem.—Geol. Soc. Am., 162:81-94.

Duncan, R.A, and Richards, M.A., 1991. Hotspots, mantle plumes, flood basalts, and true polar wander. *Rev. Geophys.,* 29:31-50.

Duque-Caro, H., 1990. Neogene stratigraphy, paleoceanography and paleobiogeography in northwest South America and the evolution of the Panama Seaway. *Palaeogeogr., Palaeoclimatol., Palaeoecol.,* 77:203-234.

Farrell, J.W., Raffi, I., Janecek, T.R., Murray, D.W., Levitan, M., Dadey, K.A., Emeis, K-C., Lyle, M., Flores, J-A., and Hovan, S., 1995. Late Neogene sedimentation patterns in the eastern equatorial Pacific Ocean. *In* Pisias, N.G., Mayer, L.A., Janecek, T.R., Palmer-Julson, A., and van Andel, T.H. (Eds.), *Proc. ODP, Sci. Results,* 138: College Station, TX (Ocean Drilling Program), 717-756.

Feldberg, M., and Mix, A.C., in press. Sea surface temperature estimates in the southeast Pacific based on planktonic foraminiferal species: modern calibration and last glacial maximum. *Mar. Micropaleontol.*

Ganeshram, R.S., Pedersen, T.F., Calvert, S.E., and Murray, J.W., 1995. Large changes in oceanic nutrient inventories from glacial to interglacial period. *Nature,* 376:755-758.

Gildor, H., and Tziperman, E., 2000. Sea ice as the glacial cycles' climate switch: role of seasonal and orbital forcing. *Paleoceanography,* 15:605-615.

Gordon, A.L., 1986. Interocean exchange of thermocline water. *J. Geophys. Res.*, 91:5037-5046.

Gregory-Wodzicki, K.M., 2000. Uplift history of the Central and Northern Andes: a review. *Geol. Soc. Am. Bull.,* 112:1091-1105.

Gripp, A.E., and Gordon, R.G., 1990. Current plate velocities relative to the hotspots incorporating the NUVEL-1 Global plate motion model. *Geophys. Res. Lett.*, 17:1109-1112.

Harris, S.E., and Mix, A.C., 1999. Pleistocene precipitation balance in the Amazon basin recorded in deep-sea sediments. *Quat, Res.,* 51:14-26.

Haug, G.H., and Tiedemann, R., 1998. Effect of the formation of the Isthmus of Panama on Atlantic Ocean thermohaline circulation. *Nature*, 393:673-676.

Haug, G.H., Tiedemann, R., Zahn, R., and Ravelo, A.C., 2001. Role of Panama Uplift on oceanic freshwater balance. *Geology,* 29:207-210.

Hebbeln, D., Wefer, G., Baltazar, M., Beese, D., Bendtsen, J., Butzin, M., Daneri, G., Dellarossa, V., Diekamp, V., Dittert, N., Donner, B., Giese, M., Glud, R., Gundersen, J., Haese, R., and Hensen, C, 1995. *Fahrtbericht zur FS Sonne fahrt SO-102, Valparaiso--Valparaiso, 9.5.-28.6.95*. Berichte aus dem Fachbereich Geowissenschaften der Universitat Bremen, 68.

Hendy, I.L., and Kennett, J.P., 1999. Latest Quaternary North Pacific surface water responses imply atmosphere-driven climate instability. *Geology,* 27:291-294.

Hendy, I.L., and Kennett, J.P., 2000. Dansgaard-Oeschger cycles and the California Current System: planktonic foraminiferal response to rapid climate change in Santa Barbara Basin, Ocean Drilling Program Hole 893A. *Paleoceanography*, 15:30-42.

Herron, E.M., Cande, S.C., and Hall, B.R., 1981. An active spreading center collides with a subduction zone: a geophysical survey of the Chile Margin triple junction. *Mem—Geol. Soc. Am.* 154:683-701.

Hey, R., Johnson, G.L., and Lowrie, A., 1977. Recent plate motions in the Galapagos area. *Geol. Soc. Am. Bull.,* 88:1385-1403.

Hooghiemstra, H., and Ran, E.T.H., 1994. Late Pliocene-Pleistocene high resolution pollen sequence of Columbia: an overview of climate change. *Quat. Intern.* 21:63-80.

Imbrie, J., Boyle, E.A., Clemens, S.C., Duffy, A., Howard, W.R., Kukla, G., Kutzbach, J., Martinson, D.G., McIntyre, A., Mix, A.C., Molfino, B., Morley, J.J., Peterson, L.C., Pisias, N.G., Prell, W.L., Raymo, M.E., Shackleton, N.J., and Toggweiler, J.R., 1993. On the structure and origin of major glaciation cycles, 2. The 100,000-year cycle. *Paleoceanography*, 8:699–736.

Imbrie, J., McIntyre, A., and Mix, A., 1989. Oceanic response to orbital forcing in the late Quaternary: observational and experimental strategies. *In* Berger, A., Schneider, S., and Duplessy, J.C. (Eds.), *Climate and GeoSciences,* Dordrecht (Kluwer Academic), 121-164.

Jasper, J., Hayes, J.M., Mix, A.C., and Prahl F.G., 1994. Photosynthetic ^{13}C fractionation and concentrations of dissolved CO_2 in the Central Equatorial Pacific during the last 255,000 years. *Paleoceanography,* 9:781-798.

Jousaumme, S., Sadourny, R., and Vignal, C., 1986. Origin of precipitating water in a numerical simulation of the July climate. *Ocean-Air Interactions,* 1:43-56.

Keigwin, L.D., and Jones, G.A., 1990. Deglacial climatic oscillations in the Gulf of California. *Palecoceanograaphy*, 5:1009-1023.

Kemp, A.E.S., Baldauf, J.G., and Pearce, R.B., 1995. Origins and Paleoceanographic significance of laminated diatom ooze from the eastern equatorial Pacific Ocean. *In* Pisias, N.G., Mayer, L.A., Janecek, T.R., Palmer-Julson, A., and van Andel, T.H. (Eds.), *Proc. ODP, Sci. Results,* 138: College Station, TX (Ocean Drilling Program), 641-645.

Kennett, J.P., 1974. Development of the Circum-Antarctic Current. *Science,* 186:144-147.

Kennett, J.P., 1977. Cenozoic evolution of Antarctic glaciation, the circum-Antarctic Ocean, and their impact on global paleoceanography. *J. Geophys. Res.,* 82:3843-3860.

Kennett, J.P., and Ingram, B.L., 1995. A 20,000-year record of ocean circulation and climate change from the Santa Barbara basin. *Nature*, 377:510-513.

Kennett, J.P., and Shackleton, N.J., 1976. Oxygen isotopic evidence for the development of the psychrosphere 38 Myr ago. *Nature,* 260:513-515.

Kroopnick, P.M., 1985. The distribution of ^{13}C of ΣCO_2 in the world oceans. *Deep-Sea Res.,* Part A, 32:57-84.

Labeyrie, L., and Elliot, M., 1999. Abrupt climatic changes – causes and consequences: an introduction. *In* Abrantes F., and Mix, A. (Eds.), *Reconstructing Ocean History, A Window into the Future*. New York (Kluwer Press), 73-82.

Lamy, F., Hebbeln, D., and Wefer, G., 1999. High-resolution marine record of climatic change in mid-latitude Chile during the last 28,000 years based on terrigenous sediment parameters. *Quat. Res.,* 51:83-93.

Le, J., Mix, A., and Shackleton, N.J., 1995. Late Quaternary paleoceanography in the eastern equatorial Pacific from planktonic foraminifera: a high-resolution record from Site 846. *In* Pisias, N.G., Mayer, L., Janecek, T., Palmer-Julson, A., van Andel, T.H. (Eds.), *Proc. ODP, Sci. Results,* 138: College Station, TX (Ocean Drilling Program), 675-693.

Lea, D.W., Pak, D.K., and Spero, H.J., 2000. Climate impact of late Quaternary equatorial Pacific sea surface temperature variations. *Science,* 289:1719-1724.

Levitus, S., Conkright, M.E., Reid, J.L., Najjar, R.G., and Mantyla, A., 1993. Distribution of nitrate, phosphate, and silicate in the world oceans. *Prog. Oceanogr.,* 31:245-273.

Liu, Z., and Huang, B., 2000. Cause of tropical Pacific warming trend. *Geophys. Res. Lett.,* 27:1935-1938.

Lonsdale, P., 1976. Abyssal circulation of the southeastern Pacific and some geological implications. *J. Geophys. Res.,* 81:1163-1176.

Lonsdale, P., and Klitgord, K.D., 1978. Structure and tectonic history of the eastern Panama Basin. *Geol. Soc. Amer. Bull.,* 89:981-999.

Loubere, P., 2000. Marine control of biological production in the eastern equatorial Pacific Ocean. *Nature,* 406:497-500.

Lowell, T.V., Heusser, C.J., Andersen, B.G., Moreno, P.I., Hauser, A., Heusser, L.E., Schlüchter, C., Marchant, D.R., Denton, G.H., 1995. Interhemispheric correlation of late Pleistocene glacial events. *Science,* 269:1541-1549.

Lund, D.C., and Mix, A.C., 1998. Millennial-scale deep water oscillations: reflections of the North Atlantic in the deep Pacific from 10 to 60 Ka. *Paleoceanography,* 13:10-19.

Lyle, M., Murray, D.W., Finney, B.P., Dymond, J., Robbins, J.M., and Brooksforce, K., 1988. The record of late Pleistocene biogenic sedimentation in the eastern tropical Pacific Ocean. *Paleoceanography,* 3:39-59.

Maasch, K.A., and Saltzman, B., 1990. A low-order dynamical model of global climatic variability over the full Pleistocene. *J. Geophys. Res.,* 95:1955-1963.

MacAyeal, D., 1993. Binge/purge oscillations of the Laurentide Ice Sheet as a cause of the North Atlantic's Heinrich events. *Paleoceanography,* 8:775-784.

Magaña, V., Amador, J.A., and Medina, S., 1999. The midsummer drought over Mexico and Central America. *J. Climate,* 12:1577-1588.

Martinez-Pardo, R., 1990. Major Neogene events of the Southeastern Pacific: the Chilean and Peruvian record. *Palaeogeogr., Palaeoclimatol., Palaeoecol.,* 77:263-278.

Mayer, L.A., Shipley, T.H., and Winterer, E.L., 1986. Equatorial Pacific seismic reflectors as indicators of global oceanographic events. *Science,* 233:761-764.

McIntyre, A., and Molfino, B., 1996. Forcing of Atlantic equatorial and subpolar millennial cycles by precession. *Science,* 274:1867-1870.

McIntyre, A., Ruddiman, W.F., Karlin, K., and Mix, A.C., 1989. Surface water response of the equatorial Atlantic Ocean to orbital forcing. *Paleoceanography*, 4:19-55.

Mikolajewicz, U., and Crowley, T.J., 1997. Response of a coupled ocean/energy balance model to restricted flow through the central American Isthmus. *Paleoceanography,* 12:429-441.

Mikolajewicz, U., Crowley, T.J., Schiller, A., and Voss, R., 1997. Modelling teleconnections between the North Atlantic and North Pacific during the Younger Dryas. *Nature,* 387:384-387.

Mikolajewicz, U., Maier-Reimer, E., Crowley, T.J., and Kim, K.-Y., 1993. Effect of Drake and Panamanian gateways on the circulation of an ocean model. *Paleoceanography,* 8:409-426.

Mix, A.C., 1989. Influence of productivity variations on long-term atmospheric CO_2. *Nature,* 337:541-544.

Mix, A.C., Le, J., and Shackleton, N.J., 1995. Benthic foraminifer stable isotope stratigraphy of Site 846: 0-1.8 Ma. *In* Pisias, N.G., Mayer, L.A., Janecek, T.R., Palmer-Julson, A., and van Andel, T.H. (Eds.), *Proc. ODP, Sci. Results,* 138: College Station, TX (Ocean Drilling Program), 839-854.

Mix, A.C., Lund, D.C., Pisias, N.G., Bodén, P., Bornmalm, L., Lyle, M., Pike, J., 1999a. Rapid climate oscillations in the northeast Pacific during the last deglaciation reflect northern and southern hemisphere sources. *In* Clark, P.U., Webb, R.S., and Keigwin, L.D. (Eds.), *Mechanisms of Global Climate Change at Millennial Time Scales:* Geophys. Monogr., Am. Geophys. Union, 112:127-148.

Mix, A.C., Morey, A.E., Pisias, N.G., Hostetler, S., 1999b. Foraminiferal faunal estimates of paleotemperatures: circumventing the no-analog problems yields cool ice-age tropics. *Paleoceanography,* 14:350-359

Muller R.A., and MacDonald, G.J., 1997. Glacial cycles and astronomical forcing. *Science,* 277:215-218.

Ninkovich, D., and Shackleton, N.J., 1975. Distribution, stratigraphic position and age of ash layer "L," in the Panama Basin Region. *Earth Planet. Sci. Lett.,* 27:20-34.

Oberhänsli, H., Heinze, P., Diester-Haass, L., and Wefer, G., 1990. Upwelling off Peru during the last 430,000 yr and its relationship to the bottom-water environment, as deduced from coarse grain-size distributions and analyses of benthic foraminifers at Holes 679D, 680B, and 681B, Leg 112. *In* Suess, E., von Huene, R., et al., *Proc. ODP, Sci. Results,* 112: College Station, TX (Ocean Drilling Program), 369-390.

Phleger, F.B., and Soutar, A., 1973. Production of benthic foraminifera in three east Pacific oxygen minima. *Micropaleontology*, 19:110-115.

Pinot, S., Ramstein G., Harrison, S.P., Prentice, I.C., Guiot, J., Stute, M., and Joussaume, S., 1999. Tropical paleoclimates at the Last Glacial Maximum: comparison of Paleoclimate Modeling Intercomparison Project (PMIP) simulations and paleodata. *Climate Dynamics,* 15:857-874.

Pisias, N.G., Mayer, L.A., and Mix, A.C., 1995. Paleoceanography of the eastern equatorial Pacific during the Neogene: synthesis of Leg 138 drilling results. *In* Pisias, N.G., Mayer, L.A., Janecek, T.R., Palmer-Julson, A., and van Andel, T.H. (Eds.), *Proc. ODP, Sci. Results,* 138: College Station, TX (Ocean Drilling Program), 5-21.

Pisias, N.G., and Mix, 1997, A.C., 1997. Spatial and temporal oceanographic variability of the eastern equatorial Pacific during the late Pleistocene: evidence from radiolaria microfossils. *Paleoceanography,* 12:381-393

Rahmstorf, S., 1995. Bifurcations of the Atlantic thermohaline circulation in response to changes in the hydrologic cycle. *Nature,* 378:145-150.

Reid, J.L., 1973. Transpacific hydrographic sections at Lats. 43S and 28S: The SCORPIO Expedition - III. Upper water and a note on southward flow at mid depth. *Deep-Sea Res.,* 20:39-50.

Rodbell, D.T., Seltzer, G.O., Anderson, D.M., Abbott, M.A., Enfield, D.B., and Newman, J.H., 1999. An ~15,000 year record of El Nino-driven alluviation in southwestern Ecuador. *Science,* 283:516-520.

Ruddiman, W.F., and M.E. Raymo, 1988. Northern hemisphere climate régimes during the past 3 Ma: possible tectonic connections. *Philos Trans. R. Soc. London B,* 318:411-430.

Strub, P.T., Mesias, J.M., Montecino, V., Rutllant, J., and Salinas, S., 1998. Coastal Ocean Circulation off Western South America. *In* Robinson, A.R., and Brink, K.H. (Eds.), *The Sea* (Coastal Oceans), v. 11, New York (Wiley), 273-313.

Talley, L.D., 1993. Distribution and formation of the North Pacific intermediate water. *J. Phys. Oceanogr.,* 23:517-537.

Tans, P.P., Fung, I.Y., and Takahashi, T., 1990. Observational constraints on the global atmospheric CO_2 budget. *Science,* 247:1431-1438.

Thompson, L.G., Davis, M.E., Mosley-Thompson, E., Sowers, T.A., Henderson, K.A., Zagorodnov, V.S., Lin, P.N., Mikhalenko, V.N., Campen, R.K., Bolzan, J.F., Cole-Dai, J., and Francou, B., 1998. A 25,000-year tropical climate history from Bolivian ice cores. *Science,* 282:1858-1864.

Toggweiler, J.R., Dixon, K., and Broecker, W.S., 1991. The Peru upwelling and ventilation of the South Pacific thermocline. *J. Geophys. Res.,* 96:20467-20497.

Toggweiler, J.R., and Samuels, B., 1993. Is the magnitude of the deep outflow from the Atlantic Ocean actually governed by southern-hemisphere winds? *In* Heimann, M. (Ed.), *The Global Carbon Cycle:* Berlin (Springer Verlag), 303-331.

Tsuchiya, M., and Talley, L.D., 1998. A Pacific hydrographic section at 88 deg W: water-property distribution. *J. Geophys. Res.,* 103(C6):12899-12918.

van Geen, A., Fairbanks, R.G., Dartnell, P., McGann, M., Gardner, J.V., and Kashgarian, M., 1996. Ventilation changes in the northeast Pacific during the last deglaciation. *Paleoceanography*, 11:519-528.

Van der Hammen, T., Werner, J.H., and Van Dommelen, H., 1973. Palynological record of the upheaval of the northern Andes: a study of the Pliocene and lower Quaternary of the Columbian Eastern Cordillera and the early evolution of its high-Andean biota. *Rev. Palaeobotany Palynology,* 16:1-122.

Wunsch, C., Hu, D.X., and Grant, B., 1983. Mass, heat, salt, and nutrient fluxes in the South Pacific Ocean. *J. Phys. Oceanogr.,* 13:725-753.

Wyrtki, K., 1962. The oxygen minimum in relation to ocean circulation. *Deep-Sea Res.,* 9:11-23.

Zaucker, F., Stocker, T.F., and Broecker, W.S., 1994. Atmospheric freshwater fluxes and their effect on the global thermohaline circulation. *J. Geophys. Res.,* 99:12443-12457.

FIGURES

Figure 1. Proposed drill sites and ports for ODP Leg 202. Large symbols with ship track indicate primary sites. Small symbols indicate optional sites to be drilled on a time-available basis.

Figure 2. Cross-section of subsurface water masses in a transect through the drilling sites, characterized by (a) dissolved oxygen (b) phosphate, and (c) salinity concentrations (Levitus et al., 1993). Bathymetry is schematic. Southward-spreading middepth waters (labeled pcw for Pacific Central Water) are characterized by relatively low oxygen and salinity and high phosphate. Northward-spreading bottom waters, below ~3 km depth starts as relatively oxygen-rich Antarctic Circumpolar Deep Water (cpdw). Northward-spreading Antarctic Intermediate Water (aaiw), above 1 km depth, his high in oxygen but is low in both phosphate and salinity. Proposed ODP drilling sites (circles) span the water masses. White circles are primary sites. White circles with diagonal slashes are the highest priority optional sites to be drilled on a time-available basis. Open circles are alternate or optional sites. gu = Gunther Undercurrent, npiw = North Pacific Intermediate Water.

Figure 3. Major near-surface current systems of the southeast Pacific eastern boundary. The Peru Current is also known as the Humboldt Current or the Peru-Chile Current. PCCC = Peru-Chile Counter Current, PUC = Peru Undercurrent (also known as the Gunther Undercurrent), PCC = Peru Coastal Current, SEC = South Equatorial Current, EUC = Equatorial Undercurrent.

Figure 4. Modern annual-average sea-surface temperatures in the southeast Pacific.

Figure 5. Modern annual average sea-surface salinities in the southeast Pacific.

Figure 6. Modern annual average sea-surface phosphate in the southeast Pacific.

Figure 7. Magnetic lineations and bathymetry from the Cocos Rise area (after Lonsdale and Klitgord, 1978), illustrating the locations of alternate sites COC-3A (solid circle = high-priority alternate), COC-2A, and COC-4A (open circle = lower-priority alternate).

Figure 8. Magnetic lineations and bathymetry from the Carnegie Ridge area (after Lonsdale and Klitgord, 1978), illustrating the locations of Sites CAR-1C, CAR-2C, and PAN-2A (solid squares = indicate top-priority sites).

Figure 9. Magnetic lineations and bathymetry from the central Nazca Plate area (after Cande and Haxby, 1991), illustrating the locations of Sites NAZCA-10A, NAZCA -14A, NAZCA-16A, NAZCA -17A, and SEPAC-9A, SEPAC-13A, and SEPAC–14A (solid squares indicate top-priority sites and open circles indicate lower-priority alternates).

Figure 10. Magnetic lineations and bathymetry from the southern Nazca plate and Antarctic plate areas (after Cande and Leslie, 1986), illustrating the locations of Sites SEPAC-5A, SEPAC-10A, and SEPAC–19A (solid circle indicates a high-priority alternate, and open circles indicate lower-priority alternates.

Figure 11. Plate tectonic backtrack of primary drill sites and high-priority alternates (see Figure 1 for site names). Large dots give modern location. Successive dots give backtrack position at 1-m.y. intervals. The number at the end of the backtrack path is the estimated basement age.

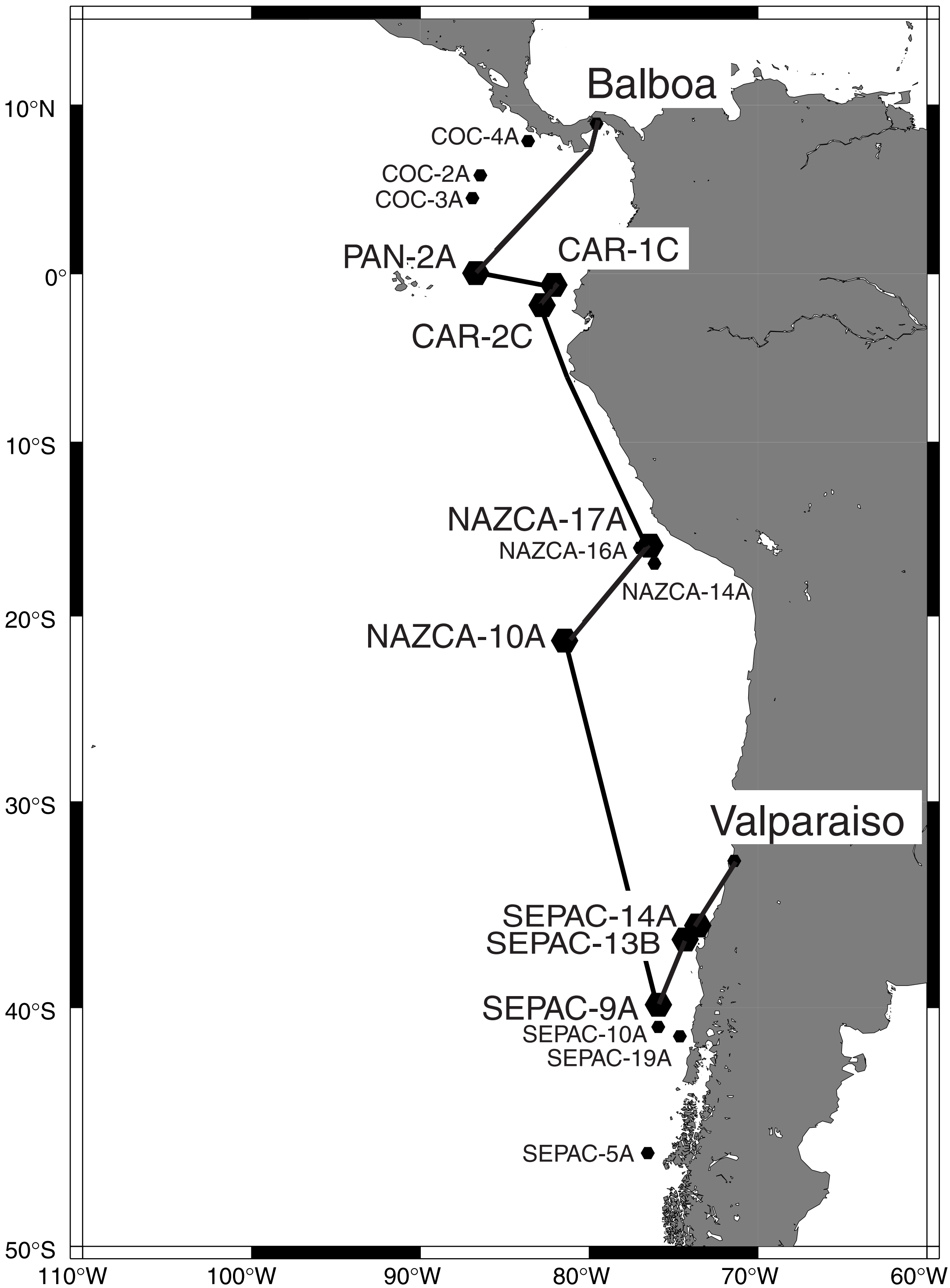
Balboa
10°N
COC-4A
COC-2A
COC-3A
PAN-2A
CAR-1C
0°
CAR-2C
10°S
NAZCA-17A
NAZCA-16A
NAZCA-14A
20°S
NAZCA-10A
30°S
Valparaiso
SEPAC-14A
SEPAC-13B
SEPAC-9A
40°S
SEPAC-10A
SEPAC-19A
SEPAC-5A
50°S
110°W
100°W
90°W
80°W
70°W
60°W

Figure 1

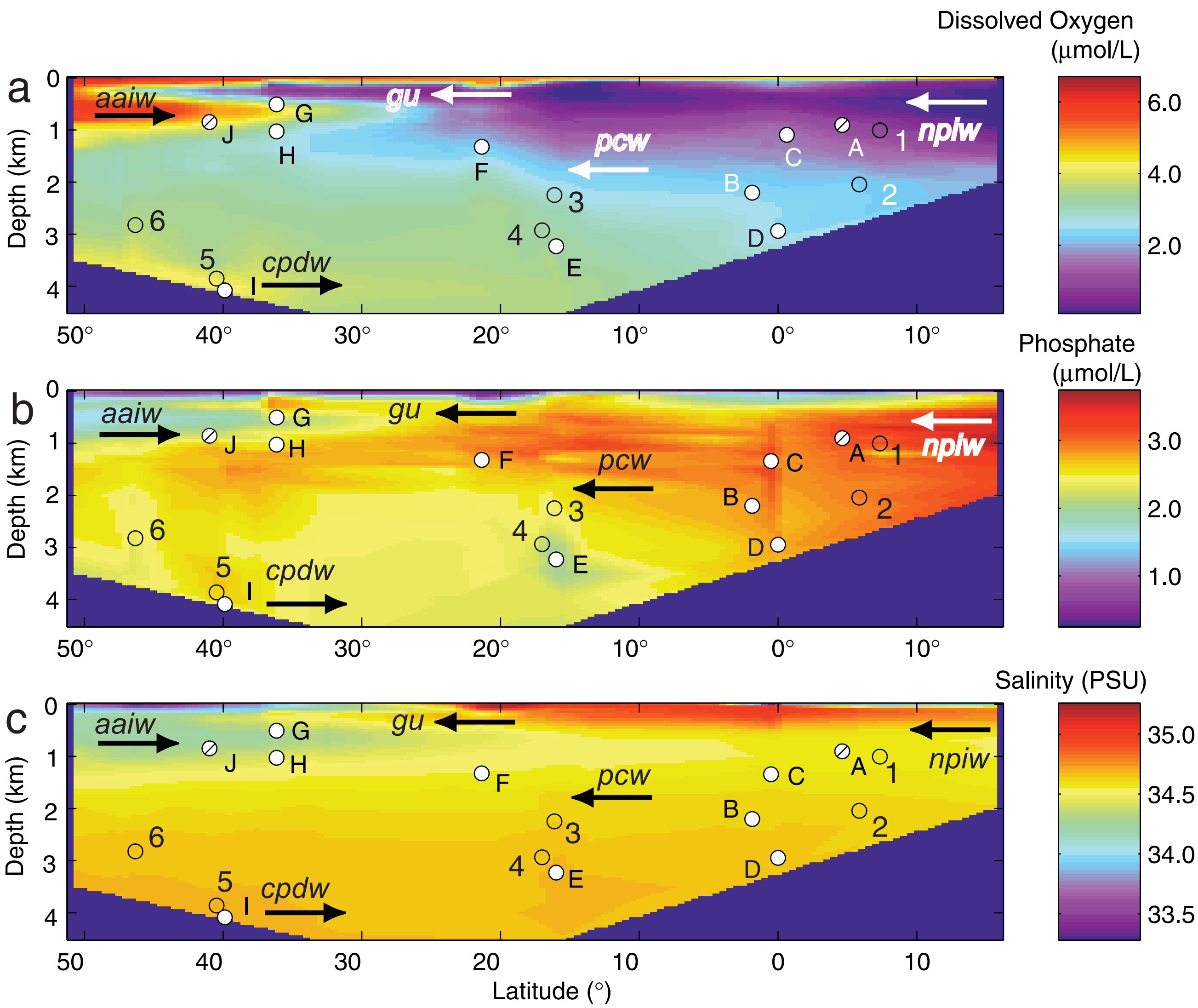
Dissolved Oxygen
(µmol/L)
6.0
4.0
2.0
a
aaiw
gu
pcw
npiw
cpdw
Depth (km)
0
1
2
3
4
A B C D E F G H I J
1 2 3 4 5 6
50°
40°
30°
20°
10°
0°
10°
Phosphate
(µmol/L)
3.0
2.0
1.0
b
aaiw
gu
pcw
npiw
cpdw
Depth (km)
Salinity (PSU)
35.0
34.5
34.0
33.5
c
aaiw
gu
pcw
npiw
cpdw
Depth (km)
50
40
30
20
10
0
10
Latitude (°)

Figure 2

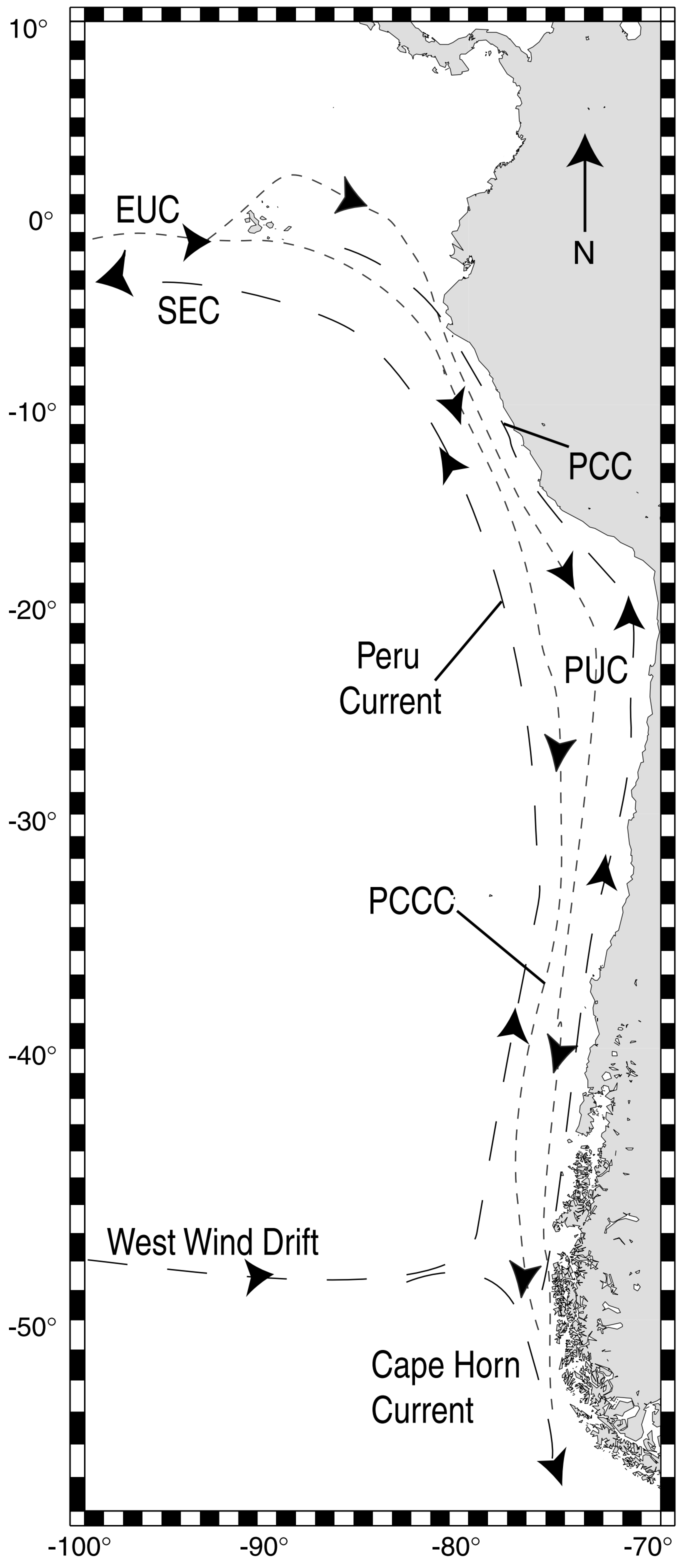
10°
0°
-10°
-20°
-30°
-40°
-50°
-100°
-90°
-80°
-70°
N
EUC
SEC
PCC
Peru
Current
PUC
PCCC
West Wind Drift
Cape Horn
Current

Figure 3

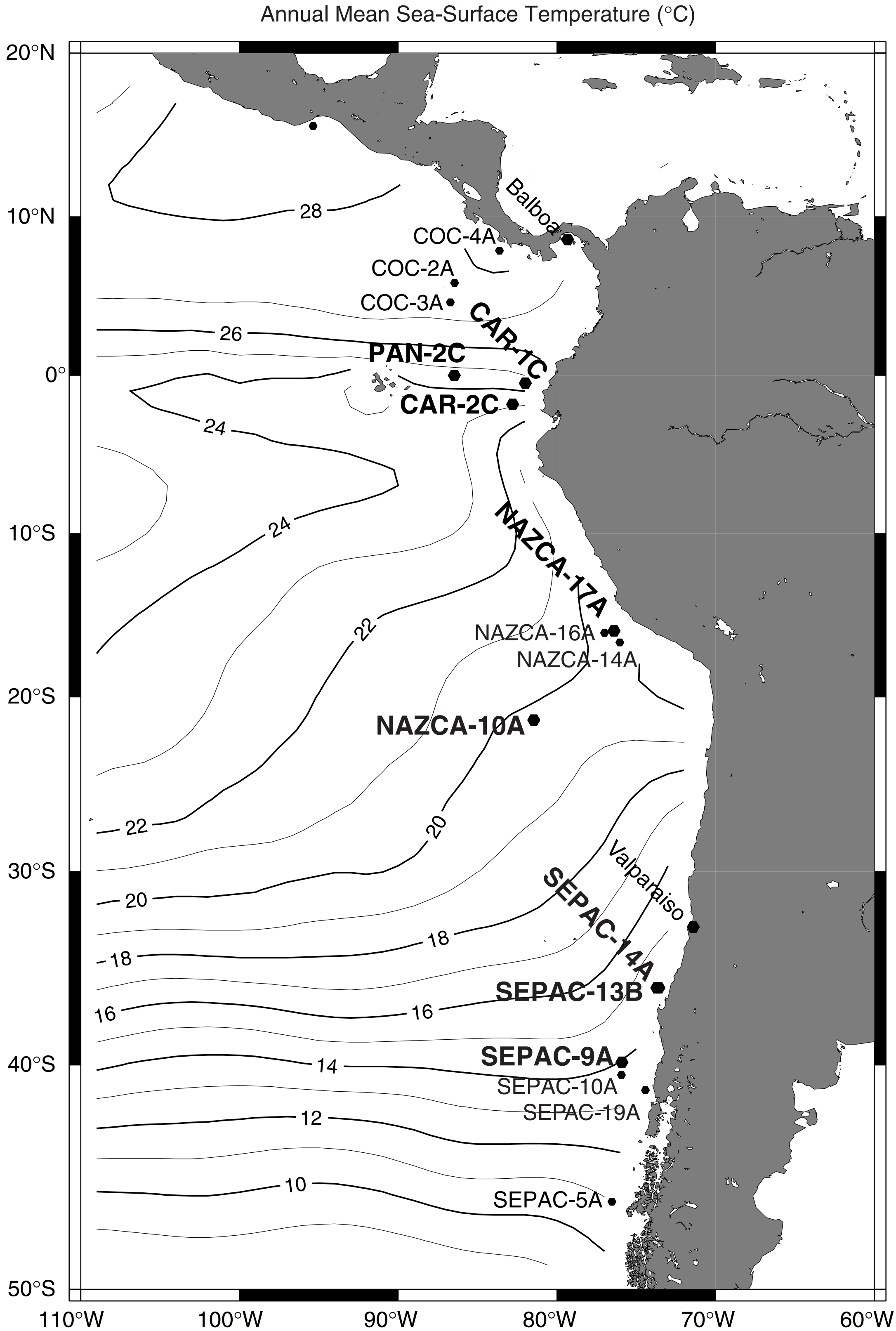
Annual Mean Sea-Surface Temperature (°C)
20°N
10°N
0°
10°S
20°S
30°S
40°S
50°S
110°W
100°W
90°W
80°W
70°W
60°W
Balboa
COC-4A
COC-2A
COC-3A
CAR-1C
PAN-2C
CAR-2C
NAZCA-17A
NAZCA-16A
NAZCA-14A
NAZCA-10A
Valparaiso
SEPAC-14A
SEPAC-13B
SEPAC-9A
SEPAC-10A
SEPAC-19A
SEPAC-5A
28
26
24
24
24
22
22
20
20
18
18
16
16
14
12
10

Figure 4

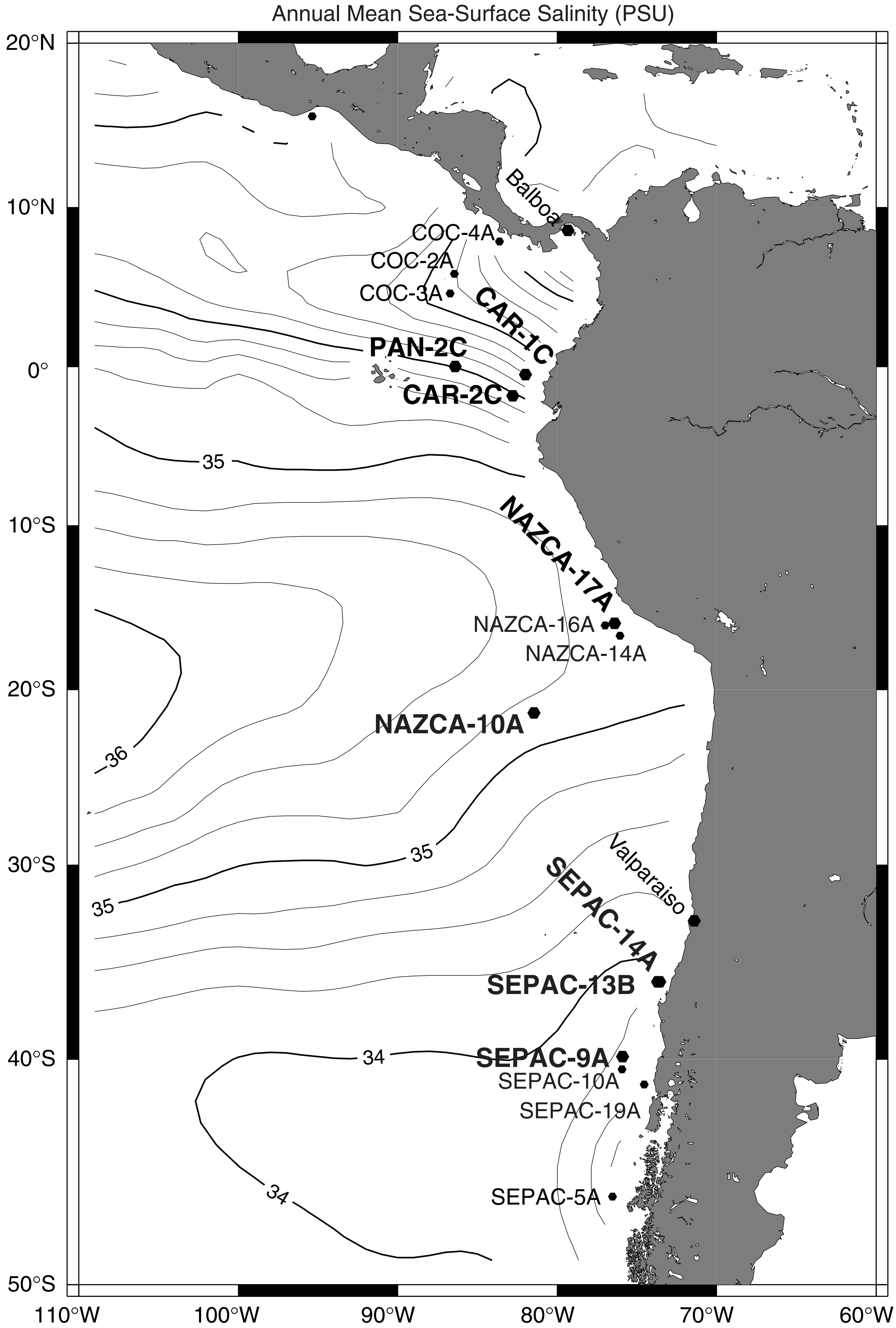
Annual Mean Sea-Surface Salinity (PSU)
20°N
10°N
0°
10°S
20°S
30°S
40°S
50°S
110°W
100°W
90°W
80°W
70°W
60°W
Balboa
COC-4A
COC-2A
COC-3A
CAR-1C
PAN-2C
CAR-2C
35
NAZCA-17A
NAZCA-16A
NAZCA-14A
NAZCA-10A
36
35
35
Valparaiso
SEPAC-14A
SEPAC-13B
34
SEPAC-9A
SEPAC-10A
SEPAC-19A
34
SEPAC-5A

Figure 5

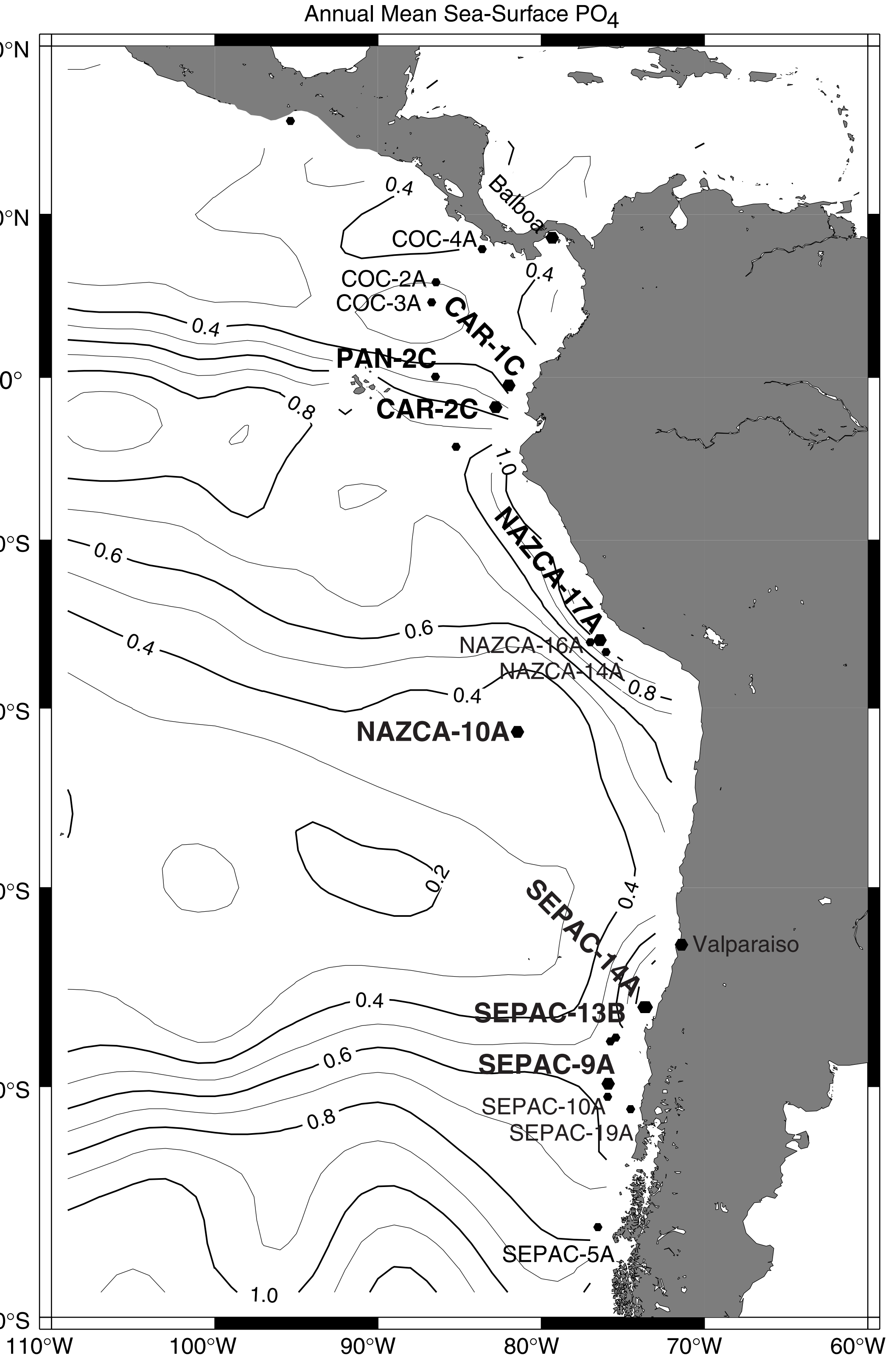
Annual Mean Sea-Surface PO4
20°N
10°N
0°
10°S
20°S
30°S
40°S
50°S
110°W
100°W
90°W
80°W
70°W
60°W
Balboa
COC-4A
COC-2A
COC-3A
CAR-1C
PAN-2C
CAR-2C
NAZCA-17A
NAZCA-16A
NAZCA-14A
NAZCA-10A
SEPAC-14A
SEPAC-13B
SEPAC-9A
SEPAC-10A
SEPAC-19A
SEPAC-5A
Valparaiso
0.2
0.4
0.6
0.8
1.0

Figure 6

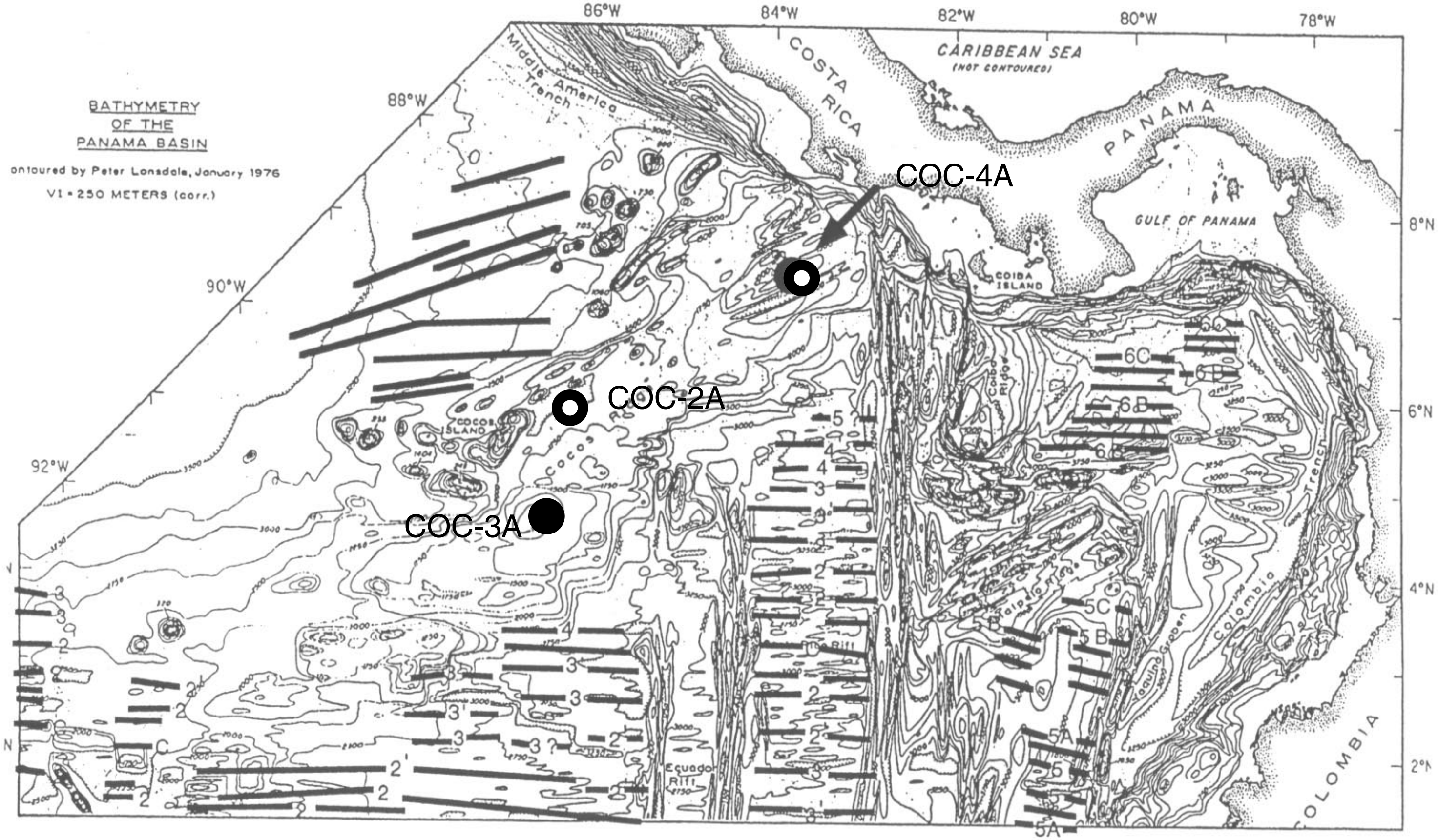
BATHYMETRY
OF THE
PANAMA BASIN
ontoured by Peter Lonsdale, January 1976
VI = 250 METERS (corr.)
86°W
84°W
82°W
80°W
78°W
88°W
90°W
92°W
8°N
6°N
4°N
2°N
CARIBBEAN SEA
(NOT CONTOURED)
COSTA RICA
PANAMA
GULF OF PANAMA
COIBA ISLAND
COLOMBIA
COCOS ISLAND
Middle America Trench
Colombia Trench
Ecuador Rift
COC-4A
COC-2A
COC-3A

Figure 7

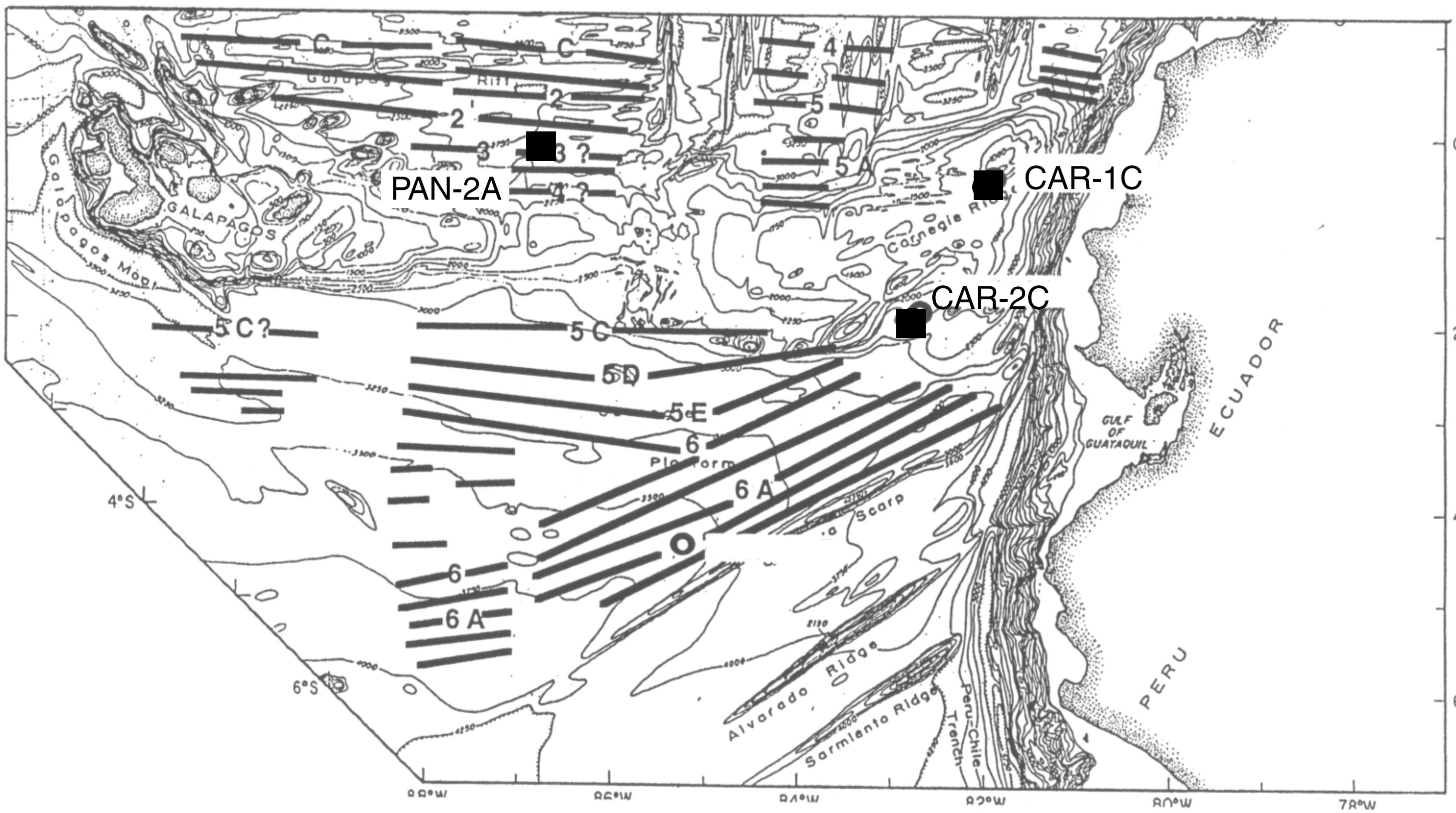
PAN-2A
CAR-1C
CAR-2C
GALAPAGOS
Carnegie Ridge
ECUADOR
PERU
GULF OF GUAYAQUIL
Alvarado Ridge
Sarmiento Ridge
Peru-Chile Trench
0°
2°S
4°S
6°S
C
2
3
4
5
5 A
5 C
5 C?
5D
5E
6
6 A
O

Figure 8

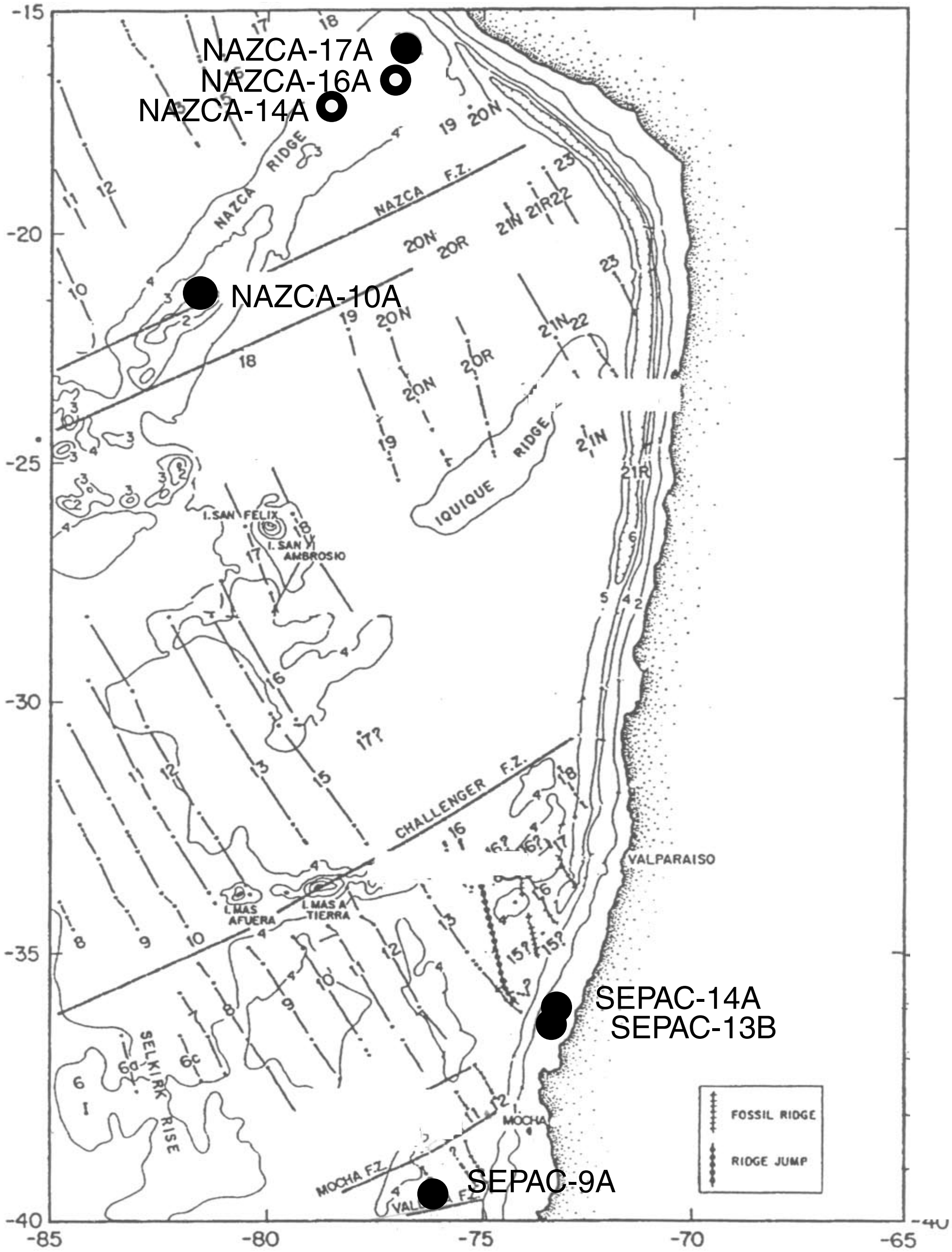
NAZCA-17A
NAZCA-16A
NAZCA-14A
NAZCA-10A
SEPAC-14A
SEPAC-13B
SEPAC-9A
NAZCA RIDGE
NAZCA F.Z.
IQUIQUE RIDGE
I. SAN FELIX
I. SAN AMBROSIO
CHALLENGER F.Z.
VALPARAISO
I. MAS AFUERA
I. MAS A TIERRA
SELKIRK RISE
MOCHA
MOCHA F.Z.
FOSSIL RIDGE
RIDGE JUMP
-15
-20
-25
-30
-35
-40
-85
-80
-75
-70
-65

Figure 9

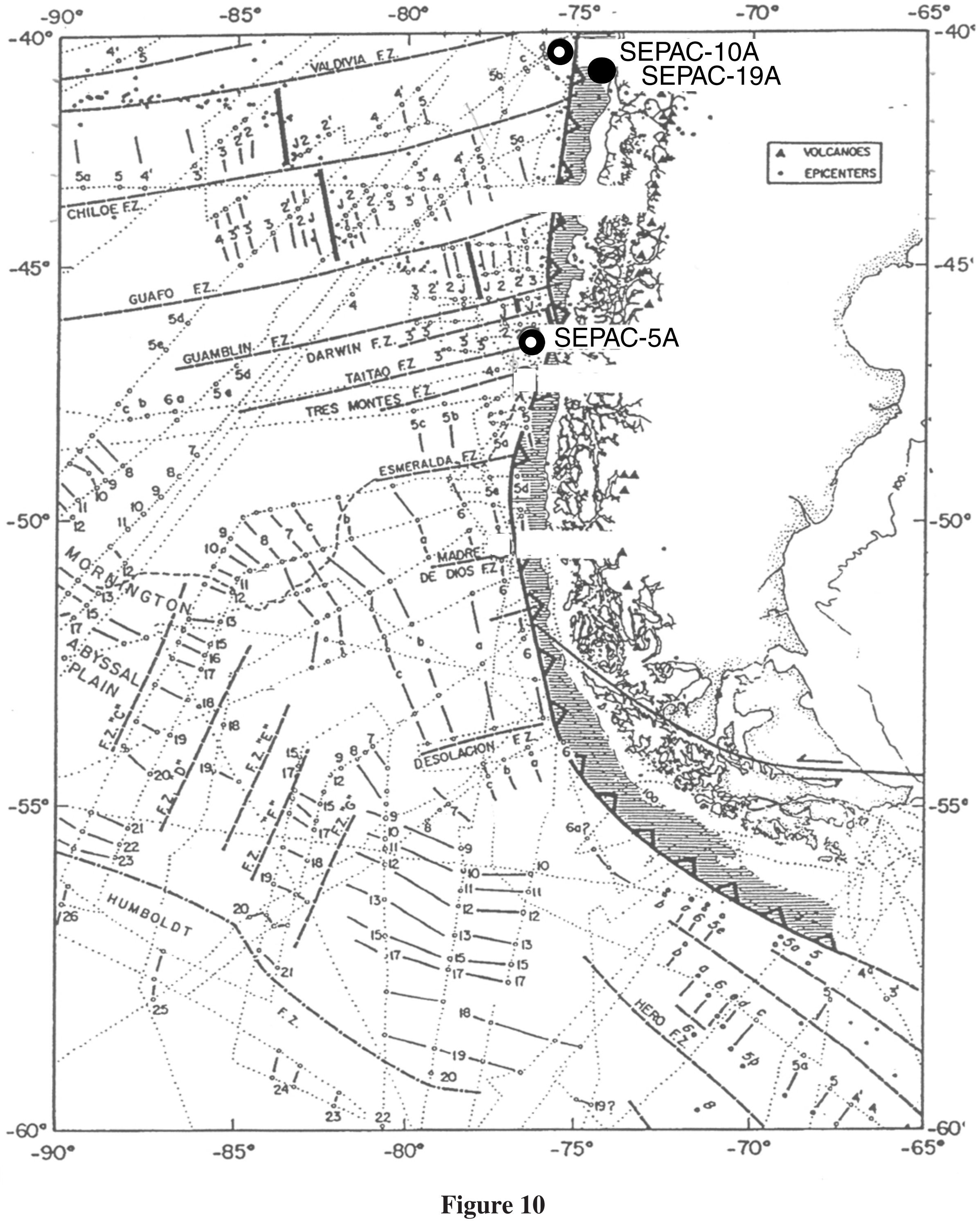
SEPAC-10A
SEPAC-19A
SEPAC-5A
VOLCANOES
EPICENTERS
VALDIVIA F.Z.
CHILOE F.Z.
GUAFO F.Z.
GUAMBLIN F.Z.
DARWIN F.Z.
TAITAO F.Z.
TRES MONTES F.Z.
ESMERALDA F.Z.
MADRE DE DIOS F.Z.
DESOLACION F.Z.
MORNINGTON ABYSSAL PLAIN
HUMBOLDT F.Z.
HERO F.Z.
F.Z. "C"
F.Z. "D"
F.Z. "E"
F.Z. "F"
F.Z. "G"
-90°
-85°
-80°
-75°
-70°
-65°
-40°
-45°
-50°
-55°
-60°

Figure 10

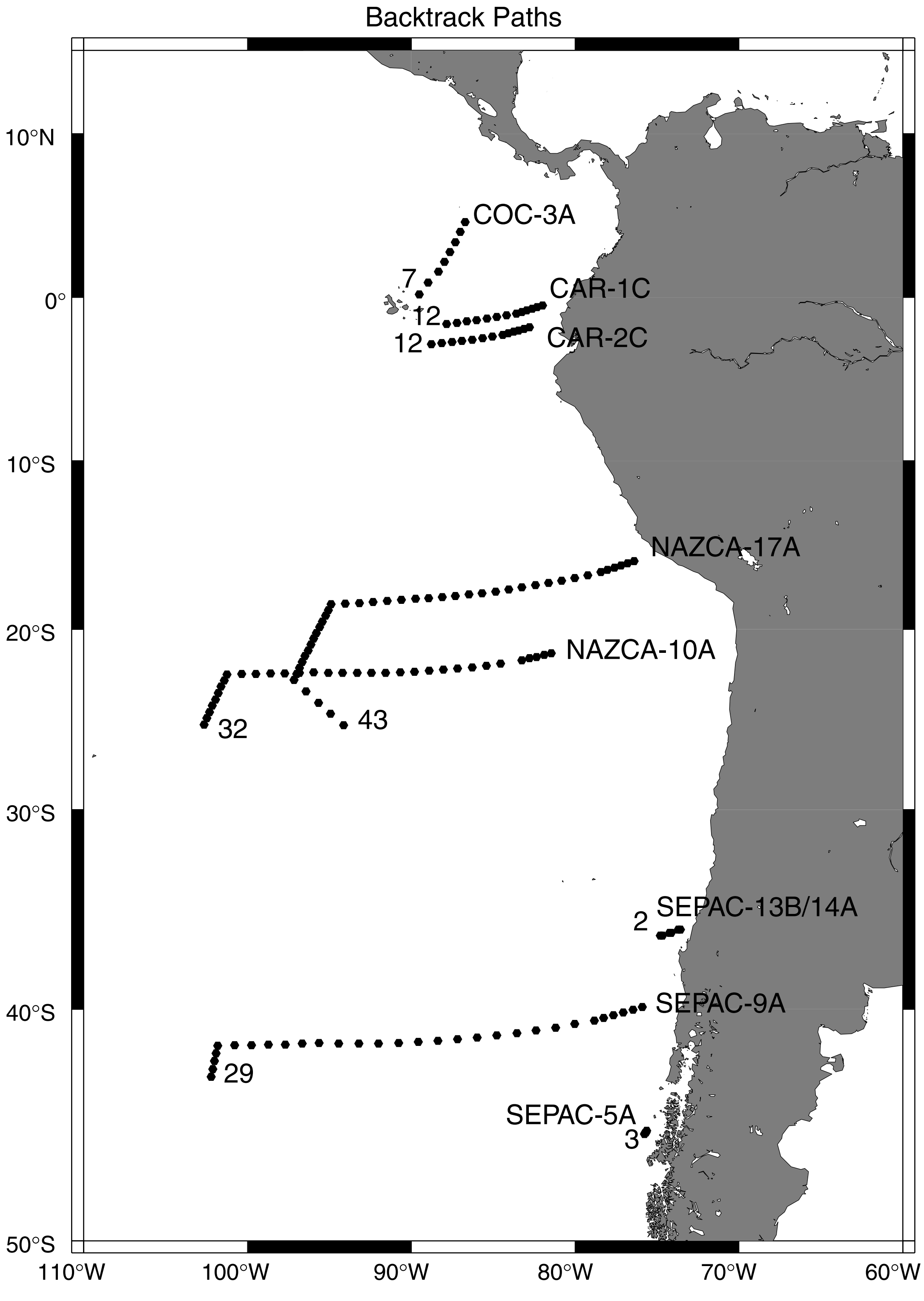
Backtrack Paths
10°N
0°
10°S
20°S
30°S
40°S
50°S
110°W
100°W
90°W
80°W
70°W
60°W
COC-3A
7
CAR-1C
12
12
CAR-2C
NAZCA-17A
NAZCA-10A
32
43
SEPAC-13B/14A
2
SEPAC-9A
29
SEPAC-5A
3

Figure 11

Table 1. Leg 202-Southeast Pacific Paleoceanographic Transects

Primary Sites Operations Plan and Time Estimate

Site No.	Location Lat/Long	Water Depth (m)	Operations Description	Transit (days)	Drilling (days)	Logging (days)	Total On-site
Valparaiso			Transit 210 nmi from Valparaiso to Site SEPAC-14A @ 10.5 kt	**0.9**			
			Survey	**0.3**			
SEPAC-14A	36°10.32'S	509	3XAPC to 150 mbsf, XCB to 200 mbsf with XCB.		**2.1**		
	73°34.32'W		Orientation on all APC cores, 4 APCT				**2.1**
			Transit 7 nmi from Site SEPAC-14A to Site SEPAC-13A @ 10.5 kt	**0.0**			
SEPAC-13B	36°14.80'S	1040	3XAPC to 150 mbsf, XCB to 200 mbsf with XCB.		**2.6**		
	73°41.06'W		Orientation on all APC cores, 4 APCT				**2.6**
			Transit 242 nmi from SEPAC-13B to SEPAC-9A @ 10.5 kt	**1.0**			
SEPAC-9A	39°53.28'S	4087	3XAPC to 150 mbsf. Deepen Hole A to 500 mbsf with XCB.		**6.9**		
	75°53.28'W		Orientation on all APC cores, 4 APCT				
			Logging Estimate from LDEO (Ule)			**1.2**	**8.1**
			Transit 1147 nmi from SEPAC-9A to NAZCA-10A @ 10.5 kt	**4.6**			
NAZCA-10A	21°21.54'S	1323	3XAPC to 150 mbsf. Deepen Hole A to 250 mbsf with XCB.		**2.9**		
	81°26.16'W		Orientation on all APC cores, 4 APCT				**2.9**
			Transit 431 nmi from NAZCA-10A to NAZCA-17A @ 10.5 kt	**1.7**			
NAZCA-17A	16°00.42'S	3228	3XAPC to 150 mbsf. Deepen Hole A to 300 mbsf with XCB.		**4.6**		
	76°22.68'W		Orientation on all APC cores, 4 APCT				
			Logging Estimate from LDEO (Ule)			**0.9**	**5.5**
			Transit 928 nmi from NAZCA-17A to CAR-2C @ 10.5 kt	**3.7**			
CAR-2C	01°52.31'S	2223	3XAPC to 150 mbsf. Deepen Hole A to 500 mbsf with XCB.		**5.0**		
	82°46.94'W		Orientation on all APC cores, 4 APCT				
			Logging Estimate from LDEO (Ule)			**1.0**	**6.0**
			Transit 84 nmi from CAR-2C to CAR-1C @ 10.5 kt	**0.3**			
CAR-1C	00°40.32'S	1423	3XAPC to 150 mbsf. Deepen Hole A to 550 mbsf with XCB.		**4.7**		
	82°04.85'W		Orientation on all APC cores, 4 APCT				
			Logging Estimate from LDEO (Ule)			**1.0**	**5.7**
			Transit 281 nmi from CAR-2C to PAN-2A @ 10.5 kt	**1.1**			
PAN-2A	00°01.31'N	2941	3XAPC to 150 mbsf. Deepen Hole A to 300 mbsf with XCB.		**4.3**		
	86°42.33'W		Orientation on all APC cores, 4 APCT				
			Logging Estimate from LDEO (Ule)			**0.9**	**5.2**
Balboa			Transit 677 nmi from PAN-2A to Balboa @ 10.5 kt	**2.7**			
				16.3	**33.1**	**5.0**	**38.1**
				TOTAL DAYS:			**54.4**

Table 2. Leg 202-Southeast Pacific Paleoceanographic Transects

Alternate Sites Operations Plan and Time Estimate

Site No.	Location Lat/Long	Water Depth (m)	Operations Description	Transit (days)	Drilling (days)	Logging (days)	Total On-site
SEPAC-19A	41°00.00'S	851	3XAPC to 80 mbsf.		1.2		
	74°27.00'W		Orientation on all APC cores, 4 APCT				
SEPAC-10A	40°28.98'S	3858	3XAPC to 150 mbsf. Deepen Hole A to 350 mbsf with XCB.		5.5		
	75°54.96'W		Orientation on all APC cores, 4 APCT				
			Logging Estimate from LDEO (Ule)			1.0	
SEPAC-5A	46°19.02'S	2825	3XAPC to 150 mbsf. Deepen Hole A to 350 mbsf with XCB.		4.6		
	76°32.28'W		Orientation on all APC cores, 4 APCT				
			Logging Estimate from LDEO (Ule)			0.9	
NAZCA-14A	17°02.10'S	2930	3XAPC to 150 mbsf. Deepen Hole A to 350 mbsf with XCB.		4.6		
	78°06.54'W		Orientation on all APC cores, 4 APCT				
			Logging Estimate from LDEO (Ule)			0.9	
NAZCA-16A	16°08.04'S	2244	3XAPC to 150 mbsf. Deepen Hole A to 350 mbsf with XCB.		4.0		
	76°58.62'W		Orientation on all APC cores, 4 APCT				
			Logging Estimate from LDEO (Ule)			0.9	
COC-3A	04°37.09'N	919	3XAPC to 150 mbsf. Deepen Hole A to 250 mbsf with XCB.		2.0		
	86°42.33'W		Orientation on all APC cores, 4 APCT				
COC-2A	05°50.57'N	2042	3XAPC to 150 mbsf. Deepen Hole A to 250 mbsf with XCB.		4.6		
	86°26.67'W		Orientation on all APC cores, 4 APCT				
			Logging Estimate from LDEO (Ule)			0.9	
COC-4A	07°51.35'N	1370	3XAPC to 150 mbsf. Deepen Hole A to 250 mbsf with XCB.		2.7		
	83°36.40'W		Orientation on all APC cores, 4 APCT				

Table 3. Absolute poles of rotation for plates in the southeast Pacific.

Plate	Rotation Start (Ma)	Interval End (Ma)	Latitude (+ = N)	Longitude (+ = E)	Ω (°/m.y.)	Ref
Antarctic	0	5	-21.5	-104.5	0.054	1
Antarctic	5	10	-21.5	-104.5	0.106	1
Antarctic	10	20	-21.5	-104.5	0.105	1
Nazca	0	5	41.9	-99.0	-0.470	2
Nazca	5	19	40.1	-93.3	-0.916	2
Nazca	19	25	67.2	-102.2	-0.815	3
Nazca	25	38	32.9	141.6	-0.469	3
Nazca	38	42	31.9	-45.8	0.975	3
Cocos	0	5	16.8	-115.9	-1.336	2
Cocos	5	10	19.1	-108.5	-2.052	2
S.America	0	11	58.7	-45.3	0.191	4
S.America	11	21	63.7	51.66	0.143	4
S.America	21	36	68.8	47.6	0.308	4
S.America	36	42	57.2	-27.3	0.213	4

[1]Cox, A., and Engebretson, D., 1985.
[2]Pisias, et al., 1995.
[3]Duncan, R.A., and Hargraves, R.B., 1984.
[4]Duncan, R.A, and Richards, M.A., 1991.